Identification of Celastramycin as a Novel Therapeutic Agent for Pulmonary Arterial Hypertension
-High-throughput Screening of 5,562 Compounds-

Ryo Kurosawa[1,2]; Kimio Satoh[1]; Nobuhiro Kikuchi[1]; Haruhisa Kikuchi[3]; Daisuke Saigusa[4]; Elias A. Mamun[1]; Mohammad A. H. Siddique[1]; Junichi Omura[1]; Taijyu Satoh[1]; Shinichiro Sunamura[1]; Masamichi Nogi[1]; Kazuhiko Numano[1]; Satoshi Miyata[1]; Akira Uruno[4]; Kuniyuki Kano[3]; Yotaro Matsumoto[3]; Takayuki Doi[3]; Junken Aoki[3];Yoshiteru Oshima[3]; Masayuki Yamamoto[4]; Hiroaki Shimokawa[1]

[1]Department of Cardiovascular Medicine, Tohoku University Graduate School of Medicine, Sendai, Japan; [2]Research Fellow of Japan Society for the Promotion of Science, Tokyo, Japan; [3]Tohoku University Graduate School of Pharmaceutical Sciences, Sendai, Japan; [4]Department of Medical Biochemistry, Tohoku University Graduate School of Medicine, Sendai, Japan

Running title: Celastramycin Ameliorates Pulmonary Hypertension

Subject Terms:
Basic Science Research
Inflammation
Metabolism
Pulmonary Hypertension
Smooth Muscle Proliferation and Differentiation

Address correspondence to:
Dr. Hiroaki Shimokawa
Professor and Chairman
Department of Cardiovascular Medicine
Tohoku University Graduate School of Medicine
1-1 Seiryo-machi, Aoba-ku
Sendai 980-8574, Japan
Tel: +81-22-717-7151
shimo@cardio.med.tohoku.ac.jp

ABSTRACT

Rationale: Pulmonary arterial hypertension (PAH) is characterized by enhanced proliferation of pulmonary artery smooth muscle cells (PASMCs) accompanying increased production of inflammatory factors and adaptation of the mitochondrial metabolism to a hyperproliferative state. However, all the drugs in clinical use target pulmonary vascular dilatation, which may not be effective for patients with advanced PAH.

Objective: We aimed to discover a novel drug for PAH that inhibits PASMC proliferation.

***Methods and Results*:** We screened 5,562 compounds from original library using high-throughput screening system to discover compounds which inhibit proliferation of PASMCs from patients with PAH (PAH-PASMCs). We found that celastramycin, a benzoyl pyrrole-type compound originally found in a bacteria extract, inhibited the proliferation of PAH-PASMCs in a dose-dependent manner with relatively small effects on PASMCs from healthy donors. Then, we made 25 analogues of celastramycin, and selected the lead compound which significantly inhibited cell proliferation of PAH-PASMCs and reduced cytosolic reactive oxygen species (ROS) levels. Mechanistic analysis demonstrated that celastramycin reduced the protein levels of hypoxia-inducible factor-1α, which impairs aerobic metabolism, and nuclear factor-κB, which induces pro-inflammatory signals, in PAH-PASMCs, leading to reduced secretion of inflammatory cytokine. Importantly, celastramycin treatment reduced ROS levels in PAH-PASMCs with increased protein levels of NF-E2-related factor 2, a master regulator of cellular response against oxidative stress. Furthermore, celastramycin treatment improved mitochondrial energy metabolism with recovered mitochondrial network formation in PAH-PASMCs. Moreover, these celastramycin-mediated effects were regulated by zinc finger C3H1 domain-containing protein, a binding partner of celastramycin. Finally, celastramycin treatment ameliorated pulmonary hypertension in three experimental animal models, accompanied by reduced inflammatory changes in the lungs.

Conclusions: These results indicate that celastramycin ameliorates pulmonary hypertension, reducing excessive proliferation of PAH-PASMCs with less inflammation and ROS levels and recovered mitochondrial energy metabolism. Thus, celastramycin is a novel drug for PAH that targets anti-proliferative effects on PAH-PASMCs.

Key Words:
Pulmonary hypertension; pulmonary circulation; proliferation; celastramycin.

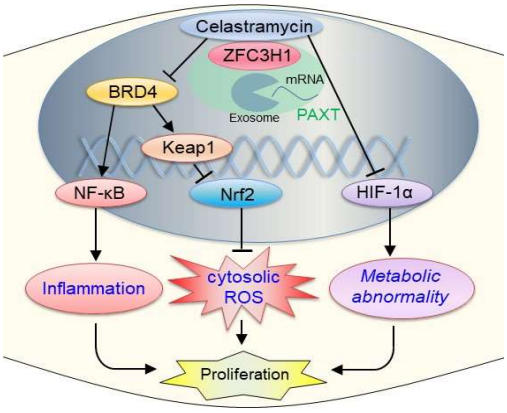

Nonstandard Abbreviations and Acronyms:

BRD4	bromodomain-containing protein 4
CEL	celastramycin
DDI	Drug Discovery Initiative
ECAR	extracellular acidification rate
HIF-1α	hypoxia-inducible factor 1α
Keap1	Kelch-like ECH-associated protein 1
NF-κB	nuclear factor-κB
NRCMs	neonatal rat cardiomyocytes
Nrf2	NF-E2-related factor 2
OCR	oxygen consumption rate
PAECs	pulmonary artery endothelial cells
PAH	pulmonary arterial hypertension
PASMCs	pulmonary artery smooth muscle cells
PAH-PAECs	PAECs from patients with PAH
PAH-PASMCs	PASMCs from patients with PAH
PAXT	poly(A) tail exosome targeting
PH	pulmonary hypertension
ROS	reactive oxygen species
RVH	right ventricular hypertrophy
RVSP	right ventricular systolic pressure
ZFC3H1	zinc finger C3H1 domain-containing protein

INTRODUCTION

Pulmonary arterial hypertension (PAH) is a fatal disease characterized by progressive obliteration of the vessel lumen and increased pulmonary artery (PA) pressure, leading to right ventricular (RV) failure and premature death.[1] During the past few decades, increased understanding of PAH pathophysiology has led to the development of several effective therapies, including prostacyclin (PGI_2) analogues and derivatives, endothelin receptor antagonists, phosphodiesterase type 5 (PDE5) inhibitors, and a soluble guanylate cyclase (sGC) stimulator.[2,3] However, all the drugs in clinical use for PAH are essentially pulmonary vasodilators, which have limited efficacy in patients with advanced PAH.[4] Indeed, despite the improvements in treatment options, overall survival still remains unsatisfactory.[5] Thus, it is important to develop novel drugs that possess different mechanisms of action.

It is known that the characteristics of PASMCs from patients with PAH (PAH-PASMCs) are different from those from healthy controls (control PASMCs).[1] Indeed, PAH-PASMCs rigorously and continuously proliferate like cancer cells and finally occlude the distal pulmonary resistant vessels.[6] Thus, effective treatment that achieves reverse remodeling needs to be developed for patients with advanced PAH. When we consider the abnormal phenotype of excessive proliferation[7] and apoptosis-resistance[8] in PAH-PASMCs, the abnormal phenotype itself can be a target for the development of novel drugs.[9] Recently, the Drug Discovery Initiative (DDI) has been founded in Japan as a hub of the national collaborative research network for drug discovery, which provides consultation, technical assistance, and public chemical samples to researchers who will begin chemical screening (http://www.ddi.u-tokyo.ac.jp/en/).[10] Tohoku University, a screening and library point of the DDI, has a unique library containing 5,562 original compounds and automated machines to perform high-throughput screening (http://www.pford.med.tohoku.ac.jp/index.html). Celastramycin is a benzoyl pyrrole-type compound originally found in a bacteria extract, which arose from functional screenings using an *ex vivo* culture system in Drosophila.[11,12] Celastramycin attenuates tumor necrosis factor (TNF)-α-mediated induction of interleukin (IL)-6 and IL-8 in human endothelial cells and lung cancer cells.[12,13] It is also known that inflammation promotes cell proliferation by upregulation of cytokines/chemokines and growth factors, some of which directly affect cell proliferation, migration, and differentiation of PASMCs. In animal models of pulmonary hypertension (PH), inflammation precedes vascular remodeling, suggesting that altered immunity is one of the primary events in the development of PAH.[14] Cytokines and growth factors increase reactive oxygen species (ROS), which augment inflammation again.[15] Mounting evidence has implicated oxidative stress as an important pathogenic mechanism in PAH. Additionally, most of the cytokines directly affect mitochondrial function in PASMCs.[9,16]

In the present study, we screened the original library of Tohoku University using a high-throughput screening system and discovered that celastramycin inhibits PAH-PASMC proliferation with anti-inflammatory and anti-oxidant effects, leading to the recovery of mitochondrial function and amelioration in three rodent models of PH. Our data suggest that celastramycin is a novel and promising drug for the treatment of PAH.

METHODS

Additional detailed methods are included in the online-only Data Supplement. The data that support the findings of this study are available from the corresponding author upon reasonable request.

Human lung samples.

Lung tissues were obtained from patients at the time of lung transplantation or surgery for lung cancer at a site far from the tumor margins as previously described.[17-19] All patients provided written informed consent for the use of their lung tissues for the present study.

Study approval.

All protocols using human specimens were approved by the Institutional Review Board of Tohoku University, Sendai, Japan (No. 2013-1-160). All animal experiments were performed in accordance with the protocols approved by the Tohoku University Animal Care and Use Committee (No. 2015-Kodo-007) based on the ARRIVE guideline.

High-throughput screening.

We used the original libraries of Tohoku University containing 5,562 unique compounds in the Drug Discovery Initiative (DDI) in Japan. PAH-PASMCs were used for the first (proliferation assay) and second (repeatability assays, counter assays and concentration-dependent assays) screening and control PASMCs were used for counter assay (proliferation assay). We optimized screening conditions (cell number, time-course of plating cells, and adding stimulus) beforehand. PAH-PASMCs were grown in DMEM with 10% FBS up to 80% confluency, which were plated at 1,000 cells/45μL mediums in each well of a 384-well plate (Greiner Bio-One, Austria) using the Multidrop™ Combi (Thermo Fisher Scientific, Waltham, USA). They were then placed in the automated incubator at 37°C for 24 hours. Diluted compounds (final concentration, 5 μmol/L) were added to columns of every plate by the Biomek NX^P (Beckman Coulter,

Brea, CA). The plates were incubated for additional 48 hours and evaluated by Cell Titer 96 AQueous One Solution Cell Proliferation Assay kit (Promega) and the SpectraMax Paradigm (Molecular Devices). The intra-plate and inter-plate variability showed a coefficient of variance of 5.9% and 4.0%, respectively.

Animal experiments.

All animal experiments were performed in accordance with the protocols approved by the Tohoku University Animal Care and Use Committee (No. 2015-Kodo-004) based on the ARRIVE (Animal Research: Reporting of In Vivo Experiments) guidelines and the recent recommendations with thorough randomization on the optimal preclinical studies in PAH.[20,21] All the operations and analyses were performed in a blinded manner. We selected male rats because male rats were used in most previous studies as monocrotaline-induced PH or SUGEN/hypoxia-induced PH in rats, which are evidenced by accumulated papers with PH model animals.[6,22] We were unable to conduct formal sample size and power calculations, because the primary goal of this study was to explore the effect of an intervention (celastramycin treatment) in vivo for the first time.

Statistical analyses.

All results are shown as mean±SEM. Comparisons of means between 2 groups were performed by unpaired Student's t-test for normally distributed cases, or the bootstrap method[23] for not normally distributed cases with unequal variances. Comparisons of means among three or more groups were performed by one-way or two-way ANOVA (analysis of variance) for normally distributed cases followed by the Tukey HDS (honestly significant difference) method or the Dunnett's method for multiple comparison, as appropriate. The normality of the underlying distributions was confirmed by the Shapiro-Wilk normality test. The multiplicity of the testing for not normally distributed cases was adjusted by the Holm's method for pairwise two-sample comparison.[24] Linear associations between two continuous variables were analyzed using linear regression model. The ratio of fully muscularized vessels was analyzed by the Poisson regression with the offset equals to the sum of total vessels with multcomp 1.4-6 package of R. Statistical significance was evaluated with GraphPad Prism 7.02 (GraphPad Software, Inc, La Jolla, CA), JMP 12 (SAS Institute Inc, Cary, America), or R version 3.3.2 (http://www.R-project.org/). All reported P values are 2-tailed, with a P value of less than 0.05 indicating statistical significance.[17,25]

RESULTS

Identification of Celastramycin by high-throughput screening.

To discover a novel drug for patients with severe PAH, we used the screening system of the DDI with 5,562 original compounds and derivatives in the original chemical library of Tohoku University. For the screening procedure, we established cell libraries of primary cultured PAH-PASMCs from patients undergoing lung transplantation and evaluated their inhibitory effects on cell proliferation after treatment with each compound (**Fig. 1A,** Online **Table I**). We performed high-throughput screening to identify compounds that reduced proliferation of PAH-PASMCs in a dose-dependent manner (**Fig. 1B**). In the first screening, PAH-PASMCs were incubated with each compound in 384-well plates for 24 hours. Among the compounds, we initially selected 80 that effectively inhibited PAH-PASMC proliferation (**Fig. 1C**). In the second screening, we performed repeatability assays and counter assays for the 80 compounds and selected 9 compounds that inhibited PAH-PASMC proliferation with relatively small effects on control PASMCs from healthy volunteers (**Fig. 1D,** Online **Fig. I**). Next, in the second screening, we performed a concentration-dependent assay for the 9 compounds in PAH-PASMCs and control PASMCs (**Fig. 1E**). In the process of final selection, we also considered the existing information, which includes stability, toxicity, and complexity in each compound (Online **Table II**). Thus, we finally selected celastramycin, as it has a promising structure and showed minimal effects on control PASMCs. We further confirmed the anti-proliferative effects of celastramycin on PAH-PASMCs in 6 different lines. Interestingly, inhibition rate of PAH-PASMC proliferation positively correlated with the pulmonary vascular resistance in each patient (Online **Fig. II**).

Since cardiac toxicity is an important issue when considering RV failure in PAH patients, we confirmed that celastramycin inhibits PAH-PASMC proliferation without harmful effects on human adult cardiomyocytes (Online **Fig. IIIA**). Interestingly, celastramycin treatment downregulated the expression of BNP (*NPPB*) in human adult cardiomyocytes compared with vehicle control (Online **Fig. IIIB**). In contrast, celastramycin treatment significantly upregulated the expressions of antioxidant genes, *SOD2* and *GCLC*, in human adult cardiomyocytes compared with vehicle control (Online **Fig. IIIB**). Moreover, we further performed experiments with PAECs from PAH patients (PAH-PAECs) and control PAECs (Online **Fig. IV**). Celastramycin treatment suppressed proliferation and apoptosis-resistance in PAH-PAECs with relatively small effects on control PAECs from healthy donors (Online **Fig. IV, A and B**). Indeed, it has been reported that PAH-PAECs have highly proliferative and apoptosis-resistant features that induce

occlusion of pulmonary arteries.[26] Moreover, celastramycin treatment significantly upregulated the eNOS levels which increase nitric oxide (NO) production in PAECs (Online **Fig. IVC**).

Again, a cell variability assay confirmed that celastramycin exerts anti-proliferative effects on PAH-PASMCs (**Fig. 1F**). We also found that celastramycin minimally induced apoptosis, assessed by staining with Annexin V or TUNEL in PAH-PASMCs (**Figs. 1G and** Online Fig. **V**). Thus, celastramycin is a novel drug that inhibits PAH-PASMC proliferation and induces apoptosis in a dose-dependent manner without harmful effects on normal PASMCs or cardiomyocytes.

Development of Celastramycin analogues and their structure-activity correlation.

To determine the anti-proliferative structure of the celastramycin molecule, we developed 25 analogues and examined their anti-proliferative effects on PAH-PASMCs. First, we synthesized 8 analogues with different lengths of alkyl chain (R) (**Fig. 2A**). These analogues had strong anti-proliferative effects on PAH-PASMCs (**Fig. 2B**). Interestingly, their anti-proliferative effects depended on the length of R (**Fig. 2C**). In contrast, substitution of R with a chlorine atom (**Fig. 2D**) completely abolished the anti-proliferative effects (**Fig. 2B**). Next, we introduced a single modification in the basal common structure, "e" (**Fig. 2E**), which slightly attenuated the anti-proliferative effects on PAH-PASMCs (**Fig. 2B**). Moreover, excessive modification of the basic common structure (**Fig. 2F**) completely abolished the anti-proliferative effects on PAH-PASMCs (**Fig. 2B**). These results suggest the crucial role of the basal common structure for the anti-proliferative effects on PAH-PASMCs. Importantly, celastramycin analogues with the basal common structure inhibited proliferation in different PAH-PASMC cell lines in a dose-dependent manner (Online **Fig. VI**). Finally, we evaluated the levels of cytosolic ROS after treatment with the 25 analogues and found that the analogue "b" significantly reduced ROS in PAH-PASMCs (**Fig. 2G**). Because we previously confirmed that intracellular ROS in PAH-PASMCs is increased compared with control PASMCs[19] and higher levels of cytosolic ROS are mechanistically involved in the proliferation of PAH-PASMCs,[19,27,28] we used the analogue "b" in the following experiments in vivo and in vitro.

Celastramycin improves mitochondrial energy metabolism in PAH-PASMCs.

Abnormal activation of hypoxia-inducible factor 1α (HIF-1α) in normoxia is well known in PAH-PASMCs, which augments transcription of many genes promoting pro-proliferative signals, impaired oxidative glucose metabolism, and the shift to aerobic glycolysis.[29] Interestingly, celastramycin treatment reduced HIF-1α mRNA (*HIF1A*) and increased glucose transporter 1 mRNA (*SLC2A1*) in PAH-PASMCs

compared with vehicle controls (**Fig. 3A,** Online **VIIA**). Importantly, HIF-1α was upregulated in PAH-PASMCs compared with control PASMCs, and celastramycin treatment significantly reduced protein levels of HIF-1α in PAH-PASMCs compared with vehicle controls (**Fig. 3A**). Additionally, celastramycin significantly reduced downstream pyruvate dehydrogenase lipoamide kinase isozyme 1 (PDK1), which inactivates pyruvate dehydrogenase (PDH) to converts pyruvic acid to acetyl CoA, and dynamin-1-like protein (DRP1) that promotes mitochondrial fission, both of which were upregulated in PAH-PASMCs compared with control PASMCs (**Fig. 3A**). Moreover, celastramycin significantly reduced protein levels of Kelch-like ECH-associated protein 1 (Keap1), which suppresses NF-E2-related factor 2 (Nrf2), in both PAH-PASMCs and control PASMCs (**Fig. 3B**). Consistently, celastramycin increased protein levels of Nrf2 in nuclear extracts in PAH-PASMCs compared with vehicle controls (**Fig. 3B**). Indeed, celastramycin upregulated the expression of Nrf2 (*NFE2L2*), a master regulator of cellular response against oxidative stress, and its downstream genes, NAD(P)H quinone dehydrogenase 1 (*NQO1*), heme oxygenase-1 (*HMOX1*), glutamate-cysteine ligase catalytic subunit (*GCLC*), and superoxide dismutase 2 (*SOD2*) in PAH-PASMCs compared with vehicle controls (**Fig. 3C, Online Fig VIIB**). Moreover, celastramycin significantly increased SOD2 in total cell lysates compared with vehicle controls (Online **Fig. VIIC**). Thus, we next focused on the role of celastramycin in altering the redox state in PAH-PASMCs. Indeed, we detected significantly higher levels of ROS in PAH-PASMCs compared with control PASMCs (**Fig. 3D**). However, celastramycin treatment significantly reduced cytosolic ROS in PAH-PASMCs assessed by staining with CellROX and 2,7-dichlorodihydrofluorescein (DCF) compared with vehicle controls (**Fig. 3D**, Online **Fig. VIII**). Consistently, NADPH oxidase activity was significantly higher in PAH-PASMCs compared with control PASMCs at baseline, which was significantly reduced by the celastramycin treatment (**Fig. 3E**). Here, it has been demonstrated that NADPH oxidase regulates the activities of Nrf2 in several cell lines.[30,31] Conversely, Keap1-Nrf2 pathway regulates the cytosolic ROS production through inhibition of NADPH oxidase.[32] Indeed, celastramycin significantly reduced Keap1 and increased Nrf2 in PAH-PASMCs (**Fig. 3B**). Thus, these reports and our data suggest that celastramycin downregulates Keap1 and upregulates Nrf2, contributing to the inhibition of NADPH oxidases in PAH-PASMCs. Next, to evaluate the antioxidative capacity of celastramycin, we evaluated levels of glutathione (GSH) and oxidized glutathione (GSSG). To elicit antioxidant effects, GSH is converted to oxidized glutathione (GSSG) and only free GSH has antioxidant effects. In contrast, GSSG lacks antioxidant functions and is a byproduct of the scavenging activity of GSH. Thus, GSH/GSSG ratio is important in assessing the total capacity of cytosolic ROS removal. Here, GSH/GSSG ratio was significantly downregulated in PAH-PASMCs compared with control PASMCs, both of which were significantly increased by celastramycin treatment (**Fig. 3F**). In contrast, celastramycin treatment significantly increased mitochondrial ROS (mROS) in PAH-PASMCs assessed by MitoSOX staining compared with vehicle controls (**Fig. 3G**). Here, it is well

known that dysregulated mitochondrial function and ATP production cause a decrease in the production of mROS in PAH-PASMCs.[33] Thus, we next examined the role of celastramycin on mitochondrial functions in PAH-PASMCs.

Using a Seahorse XF24-3 apparatus, which provides information on mitochondrial functions through real-time measurements of oxygen consumption rate (OCR; a marker of oxidative phosphorylation) and extracellular acidification rate (ECAR; a surrogate for glycolysis), we evaluated the effects of celastramycin treatment on control PASMCs and PAH-PASMCs (**Fig. 3H**). OCR reflects the mitochondrial respiration rate and energy production, while ECAR the rate of glycolysis. Here, we observed significantly lower levels of ATP production, maximal respiration, and OCR/ECAR ratio in PAH-PASMCs compared with control PASMCs, which were significantly increased by the celastramycin treatment (**Fig. 3I**). Furthermore, PAH-PASMCs showed significantly increased glycolysis compared with control PASMCs, which was slightly reduced by the celastramycin treatment (Online **Fig. IX**). Thus, we next examined the morphologies of mitochondria in PAH-PASMCs after celastramycin treatment for 24 hours. Importantly, celastramycin treatment showed increased mitochondrial networks assessed using a MitoTracker in PAH-PASMCs compared with vehicle controls (**Fig. 3J**, Online **Fig. X**). Additionally, celastramycin treatment showed increased mitochondrial networks assessed by transmission electron microscopy (TEM) in PAH-PASMCs compared with vehicle controls (**Fig. 3K**, **Online Fig. XI**). Consistently, celastramycin treatment significantly reduced the levels of dynamin-1-like protein (DRP1) that promotes mitochondrial fission (**Fig. 3A**). Moreover, celastramycin increased the expressions of genes for mitochondrial fusion, such as mitofusin 1 (*MFN1*), mitofusin 2 (*MFN2*), and mitochondrial elongation factor (*MIEF1*), and reduced the expressions for mitochondrial fission, such as dynamin 1-like protein (*DNM1L*), mitochondrial fission 1 protein (*FIS1*), and optic atrophy type 1 (*OPA1*) in PAH-PASMCs compared with vehicle controls (Online **Fig. VIID**). Additionally, celastramycin significantly upregulated the expressions of genes for mitochondrial biogenesis, such as peroxisome proliferator-activated receptor γ coactivator 1-α (PGC-1α) (*PPARGC1A*), mitochondrial transcription factor A (*TFAM*), and nuclear respiratory factor 1 (*NRF1*), and genes for mitochondrial function, such as peroxisome proliferator-activated receptor-α and δ (*PPARA*, *PPARD*), in PAH-PASMCs compared with vehicle controls (Online **Fig. VIIE**). These results suggest that celastramycin treatment affects the balance between mitochondrial biogenesis and functions, resulting in increased mitochondrial networks and mROS levels in PAH-PASMCs.

Celastramycin-mediated changes in metabolomics in PAH-PASMCs.

It has been reported that circulating metabolites are dramatically altered in PAH patients.[34] Additionally, metabolic profiles predicted the long-term prognosis of PAH patients, suggesting that metabolic changes could be important modifiers of disease progression.[34] Based on the celastramycin-mediated recovery in mitochondrial function, we hypothesized that celastramycin may change metabolic profiles in PAH-PASMCs and their secreted proteins. Thus, we performed metabolomic analyses to evaluate the metabolic changes in PAH-PASMCs by the treatment with celastramycin. Here, we used a broad metabolomics platform to analyze more than 400 metabolites in total cell lysates of PAH-PASMCs and compared the changes after the treatment with celastramycin (Online **Fig. XIIA**). Interestingly, we found a dramatic change in several metabolites by celastramycin treatment (Online **Fig. XIIB**). In agreement, celastramycin treatment increased the levels of metabolite in the tricarboxylic acid (TCA) cycle, such as Succinic acid, suggesting that celastramycin up-regulates mitochondrial respiration in PAH-PASMCs (Online **Fig. XIIC**). Here, we have measured the activities of the enzymes that regulate the levels of succinic acid (succinyl-CoA synthetase and succinate dehydrogenase) in PAH-PASMCs. Interestingly, celastramycin significantly increased both enzymes (Online **Fig. XIIC**). However, the extents of which were higher for succinyl-CoA synthase (+140%) than for succinate dehydrogenase complex subunit A (SDHA) (+20%) (Online **Fig. XIIC**). Thus, the increased levels of succinic acid by celastramycin can be explained, at least in part, by the increased ratio of succinyl-CoA synthetase/SDHA. Additionally, we further performed analyses of cytokines/chemokines and growth factors in conditioned medium from control PASMCs and PAH-PASMCs under the treatment with celastramycin (Online **Fig. XIID**). Importantly, celastramycin treatment significantly reduced the secretion of cytokines/chemokines and growth factors from PAH-PASMCs, which were elevated compared with control PASMCs at baseline (Online **Fig. XIID**). These results suggest that celastramycin changes the cell metabolism and reduces inflammatory cytokines/chemokines and growth factors in PAH-PASMCs.

Celastramycin inhibits inflammatory signaling in PAH-PASMCs.

Celastramycin was originally identified as a potent suppressor of immune deficiency pathways, which regulate Gram-positive bacterial infections via transcription factor NF-κB-like transcriptional factor.[11,12] Inflammation and oxidative stress are closely connected by cytokines/chemokines and growth factors.[15] Excessively augmented NF-κB expression is recognized in PAH-PASMCs and induces the transcription of many genes producing pro-proliferative and pro-inflammatory signals and impaired mitochondrial metabolism.[35] Consistent with this, knockdown of NF-κB by siRNA significantly reduced

PAH-PASMC proliferation compared with control siRNA (**Fig. 4A**). Importantly, celastramycin treatment significantly reduced protein levels of NF-κB in the nuclear extracts of PAH-PASMCs compared with vehicle controls (**Fig. 4B**). Moreover, phosphorylation of extracellular signal-regulated kinases (ERK1/2) in total cell lysates was significantly upregulated in PAH-PASMCs compared with control PASMCs, which was significantly reduced by celastramycin treatment (**Fig. 4C**). Additionally, celastramycin significantly reduced gene expression levels of NF-κB (*RELA*) and Toll-like receptor 4 (*TLR4*) compared with vehicle controls (**Fig. 4D**). These results suggest that celastramycin inhibits inflammation through suppression of TLR4-NF-κB-ERK signaling in PAH-PASMCs. Bromodomain-containing protein 4 (BRD4) is an epigenetic reader that binds to acetylated histone tails and other proteins to regulate transcription of genes involved in many cellular functions, such as cell cycle, apoptosis, and inflammation.[36] Here, protein levels of BRD4 in PAH-PASMCs was significantly upregulated compared with control PASMCs, which was significantly reduced by celastramycin treatment (**Fig. 4E**). Additionally, celastramycin treatment significantly reduced protein levels of survivin and translocation of nuclear factor of activated T cells 2 (NFATc2) to the nucleus, both of which are downstream of BRD4 and regulate the cell cycle in PAH-PASMCs (**Fig. 4E**). Here, based on the previous reports,[37,38] we hypothesized that celastramycin-mediated downregulation of BRD4 may have effects on Keap1-Nrf2 signaling. Indeed, inhibition of BRD4 by siRNA significantly reduced the expression of Keap1 (**Fig. 4F**). Altogether, celastramycin reverses altered mitochondrial metabolism and reduces inflammation and ROS production through changes in HIF-1α, NF-κB and Nrf2, leading to inhibition of excessive proliferation in PAH-PASMCs (**Fig. 4G**). Recently, there is mounting evidence that dysfunctional DNA-damage response mechanisms promote resistance to apoptosis and proliferative phenotype in PAH-PASMCs.[39] Interestingly, we found that DNA damage was significantly increased in PAH-PASMCs compared with control PASMCs, both of which were significantly reduced by celastramycin treatment in a dose-dependent manner (Online **Fig. XIIIA**). Consistently, protein levels of γH2AX were significantly reduced by celastramycin treatment (Online **Fig. XIIIB**). Indeed, PAH is characterized by elevation of circulating cytokines (e.g., IL-6) that promotes DNA damage[22] and oxidative stress that induces DNA damage through DNA base oxidation and deamination.[39] Thus, celastramycin-mediated anti-inflammatory and ani-oxidative effects may have alleviated the DNA damage especially in PAH-PASMCs. Next, we further evaluated the enzyme implicated in DNA repair, poly (ADP-ribose) polymerase-1 (PARP-1), in control PASMCs and PAH-PASMCs. However, celastramycin did not have any significant effects on the protein levels of PARP-1 (Online **Fig. XIIIB**). Altogether, celastramycin may play as a modulator of DNA damage with anti-inflammatory and anti-oxidative effects on PAH.

ZFC3H1-mediated inhibition of BRD4 and HIF-1α by Celastramycin treatment.

A recent study clearly demonstrated that zinc finger C3H1 domain-containing protein (encoded by *ZFC3H1*) is a binding partner of celastramycin.[13] Moreover, ZFC3H1 plays a crucial role in the degradation of nuclear RNAs, such as messenger RNAs, ribosomal RNAs, and non-coding RNAs, and thus regulates multiple intracellular signaling pathways.[40-42] Here, we hypothesized that celastramycin-mediated inhibitory effects on transcriptional modulators could be regulated by its binding partner, ZFC3H1. Indeed, inhibition of ZFC3H1 by siRNA significantly reduced the mRNA expression and protein levels of BRD4 (**Fig. 5A**). Additionally, inhibition of ZFC3H1 by siRNA significantly reduced the expression of HIF-1α and its downstream DRP1 (**Fig. 5B**). Moreover, inhibition of ZFC3H1 induced downregulation of Keap1 and resultant upregulation of Nrf2 and SOD2 (**Fig. 5C**). In contrast, we overexpressed ZFC3H1 in PAH-PASMCs using a ZFC3H1-encoding plasmid. Importantly, overexpression of ZFC3H1 significantly upregulated BRD4, HIF1α, DRP-1 and Keap1 (**Fig. 5D-F**). Altogether, celastramycin-mediated multiple effects can be explained by the inhibition of ZFC3H1, leading to suppression of BRD4 and HIF-1α (**Fig. 5G**). On the other hand, celastramycin significantly increased the expression of peroxisome proliferator-activated receptor γ coactivator 1-α (PGC1α) and its downstream signaling, TFAM (mitochondrial transcription factor A), PPARA (peroxisome proliferator-activated receptor-α), and PPARD (peroxisome proliferator-activated receptor-δ) in PAH-PASMCs (Online **Fig. VIIE**), which upregulate the expression of mitofusin 2 and mitochondrial biogenesis.[43] Here, we have demonstrated that AMPK plays a crucial role against the development of PAH.[18] Additionally, AMPK contributes to the activation of PGC1α and mitochondrial biogenesis,[44,45] and mROS are a physiological activator of AMPK signaling.[46] Thus, we consider that celastramycin-mediated upregulation of mROS may have activated AMPK and downstream PGC1α in PAH-PASMCs. Indeed, celastramycin treatment significantly increased the phosphorylation of AMPK, which increases the expression of PGC1α, especially in PAH-PASMCs (Online **Fig. VIIF**). Altogether, celastramycin-mediated multiple effects are based on its inhibitory effects on its binding partner, ZFC3H1 (**Fig. 5G**).[13]

Celastramycin ameliorates PH in rodent models.

Based on the celastramycin-mediated inhibitory effects on PAH-PASMC proliferation, we performed *in vivo* experiments in rodent models of PH. First, we examined the effect of celastramycin in hypoxia-induced PH in mice (**Fig. 6A**). Daily administration of celastramycin using osmotic pumps during 21 days of normoxia or chronic hypoxia had no effect on body weight or blood pressure compared with vehicle controls (**Fig. 6B, 6C**). Moreover, celastramycin treatment significantly reduced

cytokines/chemokines and growth factors in the lungs, many of which were significantly increased under hypoxia compared with normoxic controls (**Fig. 6D, Online Table III**). Importantly, celastramycin significantly reduced perivascular inflammation (Online **Fig. XIV**) and muscularization of distal pulmonary arteries (**Fig. 6E**) after hypoxic exposure compared with vehicle controls. Consistently, celastramycin significantly ameliorated hypoxia-induced increases in RVSP and RVH compared with vehicle controls (**Fig. 6F**). Next, to further assess the therapeutic potential of celastramycin for PAH, we used a model of monocrotaline-induced PH in rats (**Fig. 7A**). In this monocrotaline-induced rat model, we started celastramycin treatment during the development of PH (prevention protocol). Daily administration of celastramycin for 3 weeks had no effect on body weight or food consumption compared with vehicle controls (**Fig. 7B**). Again, consistent with the results *in vitro*, celastramycin treatment significantly reduced cytokines/chemokines and growth factors in the lung compared with vehicle controls (**Fig. 7C,** Online **Table III**). Moreover, celastramycin significantly suppressed muscularization of distal pulmonary arteries compared with vehicle controls (**Fig. 7D**). Consistently, celastramycin treatment significantly reduced RVSP and RVH compared with vehicle controls (**Fig. 7E**). Finally, to further evaluate the therapeutic potential of celastramycin for PAH, we used a third animal model of PH, in which rats were exposed to chronic hypoxia for 21 days in combination with injection of SU5416 (Sugen/hypoxia model) (**Fig. 8A**). In this Sugen/hypoxia rat model, we started celastramycin treatment after the development of PH (treatment protocol). Daily administration of celastramycin for 14 days had no effect on body weight or food consumption compared with vehicle controls (**Fig. 8B**). Protein levels of inflammatory cytokines (e.g. IL-2, IL-6) in the lungs were significantly reduced by celastramycin treatment in the Sugen/hypoxia rat model (**Figs. 8C, Online Fig XV,** Online **Table III**). Moreover, celastramycin significantly suppressed muscularization of distal pulmonary arteries compared with vehicle controls (**Fig. 8D**). Additionally, celastramycin treatment was associated with a marked reduction in proliferation and a trend for increased apoptosis in the distal pulmonary arteries in rats (Online **Fig. XVI**). Consistently, celastramycin treatment significantly reduced RVSP and RVH compared with vehicle controls (**Fig. 8E**). Importantly, celastramycin treatment significantly improved hemodynamic parameters, such as RV diastolic diameter, RV fractional area change, PA acceleration time, tricuspid annular plane systolic excursion, and cardiac output as determined by echocardiography (**Fig. 8F**). In contrast, celastramycin treatment did not change left ventricular diastolic diameter or LV ejection fraction (**Fig. 8G**). Again, we used a Seahorse XF24-3 apparatus to evaluate the mitochondrial function in cardiomyocytes using neonatal rat cardiomyocytes (NRCMs) (Online **Fig. XVIIA**). Importantly, we observed higher levels of ATP production, maximal respiration, and OCR/ECAR ratio in celastramycin-treated NRCMs compared with vehicle controls *in vitro* (Online **Fig. XVIIB, XVIIC**). Moreover, celastramycin increased the expressions of genes for mitochondrial fusion, such as mitofusin 1 (*MFN1*) and mitofusin 2 (*MFN2*), and reduced the expressions

for mitochondrial fission, such as mitochondrial fission 1 protein (*FIS1*) and mitochondrial fission 2 protein (*Mff*), and upregulated the expressions of genes for mitochondrial biogenesis, such as mitochondrial transcription factor A (*TFAM*) in NRCM compared with vehicle controls (Online **Fig. XVIID**). Here, the metabolic status of NRCMs shifted from "aerobic" to "energetic" by the OCR/ECAR analysis (Online **Fig. XVIIC**). Indeed, celastramycin treatment significantly reduced mean pulmonary arterial pressure (mPAP) and increased cardiac output (CO), resulting in the significant reduction on total pulmonary vascular resistance (TPR) compared with vehicle controls (**Fig. 8H**). Altogether, celastramycin treatment significantly improved exercise capacity and increased treadmill walking distance (**Fig. 8I**). These results suggest that celastramycin suppresses inflammation in the lungs and improves systemic metabolism, ameliorating PH and RV failure in several different animal models. Finally, we performed biochemical tests in Sugen/hypoxia-induced PH model in rats after the treatment with celastramycin or vehicle. Importantly, there was no significant change in the functions of liver and kidney, and hematology profiles after the celastramycin treatment (Online **Table** IV).

DISCUSSION

In this study, we demonstrated that celastramycin inhibits PAH-PASMC proliferation by the suppression of inflammation and oxidative stress and ameliorates PH in three different animal models. These concepts are based on the following findings; (1) we selected celastramycin as a compound that inhibits cell proliferation dose-dependently with small effects on control PASMCs, (2) celastramycin treatment increased genes for mitochondrial biogenesis and function, leading to improved mitochondrial energy metabolism and networks, (3) celastramycin significantly diminished nuclear translocation of HIF1-α and NF-κB and reduced cytokines/chemokines and growth factors, and (4) celastramycin inhibited PASMC proliferation and ameliorated PH in different animal models.

Identification of Celastramycin as a Novel Drug for PAH.

There are three main types of drugs for treating PAH, all of which aim to dilate the pulmonary arteries.[3] However, these treatments cannot stop or reverse this aggressive disease even though they help to slow its progression. Thus, patients with advanced PAH and RV failure require lung transplantation and some patients die even after the vasodilator therapy with these drugs.[4] As an additional strategy for PAH, effective treatment that achieves reverse remodeling of pulmonary arteries is warranted. Thus, we focused on the inhibition of PAH-PASMC proliferation to discover a novel drug for PAH. PAH-PASMCs have special characteristics in terms of pro-proliferative and anti-apoptotic features in common with cancer

cells.[6] The development of academic drug discovery is in response to the fact that the discovery of new drugs has come to a standstill in the pharmaceutical industry. Under these situations, the DDI was founded in Japan to promote an environment in which academic drug discovery can be performed. Using these platforms, we were able to promote drug discovery based on a clinical perspective and the knowledge of the pathogenesis of PAH. When we consider the pathological findings of PAH, actively-proliferative cell components and occlusion of the distal pulmonary arteries, it is evident that treatment with pulmonary vasodilators is useful only in patients with mild progression. In the present study, we performed phenotypic screening and discovered compounds with anti-proliferative effects on PAH-PASMCs and selected the compounds specific for the cells responsible for the disease. Then we developed 25 analogues of the hit compound to determine the lead compound, and finally selected celastramycin "b" with anti-oxidant effects for *in vivo* treatment. Finally, celastramycin was effective in three animal models of PH with no apparent side effects. This means that the anti-proliferative strategy for PASMCs may be a novel therapeutic strategy to treat PAH patients; celastramycin can be a possible drug for PAH. In the previous paper, we have already discovered sanguinarine that reduces selenoprotein P expression and PASMC proliferation and ameliorates PH in mice and rats.[19,47,48] In the present study, we used our different original library and selected celastramycin by rigorous screening to verify its safety on normal cells, which implies that celastramycin has different effects on PAH-PASMCs compared with the effects of sanguinarine-mediated inhibition of selenoprotein P.

ZFC3H1-mediated Anti-inflammatory Effects by Celastramycin.

In the present study, celastramycin inhibited NF-κB nuclear translocation and exerted anti-inflammatory effects on PAH-PASMCs *in vitro* and in rodent models of PH *in vivo*. Celastramycin is a benzoyl pyrrole-type compound originally discovered as a new antibiotic in the extract of *Streptomyces* MaB-QuH-8 from the plants of the Celastraceae in 2002.[49] Then, after searching for natural substances that regulate innate immunity using an *ex vivo* Drosophila culture system, celastramycin was identified as a potent suppressor of immune deficiency pathways, which regulate Gram-positive bacterial infections via transcription factor NF-κB-like transcriptional factor.[11,12] Thus, NF-κB-related signal transduction pathways seem to be a target for celastramycin in mammalian cells.[13] Inflammatory cytokines, such as IL-1β, IL-6, and TNF-α, are involved in NF-κB signaling and play crucial roles in the development of PAH.[50-52] Thus, the anti-inflammatory effect of celastramycin is one of its main mechanisms of action. A recent study identified that ZFC3H1, an uncharacterized zinc finger protein, is a binding partner of celastramycin, which blocks the formation of the NF-κB transcription complex.[13] Moreover, ZFC3H1 links ATP-dependent RNA helicase MTR4 with polyadenylate-binding nuclear protein 1 in the poly(A) tail exosome

targeting (PAXT) connection, which plays a crucial role in the degradation of nuclear RNAs.[40,41] Exosomes are involved in the processing of a wide range of RNAs including messenger RNAs, ribosomal RNAs, and non-coding RNAs,[42] and have been shown to regulate the production of cytokines and other inflammatory proteins.[53] Thus, celastramycin may modulate PAXT connections by binding to ZFC3H1, resulting in changes in the degradation of RNAs with inflammatory effects. Indeed, celastramycin-mediated multiple effects were due to the inhibition of ZFC3H1, leading to suppression of BRD4 and HIF-1α.

Celastramycin reduces cytosolic ROS in PAH-PASMCs

There is mounting evidence of the role of oxidative stress in the pathogenesis of PAH.[15] In the present study, celastramycin significantly reduced cytosolic ROS in PAH-PASMCs. A possible mechanism of this celastramycin-mediated reduced cytosolic ROS is the upregulation of Nrf2, which is essential for oxidative and electrophilic stress responses, and resultant downregulation of NADPH oxidase activities.[30,31] Here, it has been demonstrated that NADPH oxidase regulates the activities of Nrf2 in several cell lines.[30,31] Conversely, Keap1-Nrf2 pathway regulates the cytosolic ROS production through inhibition of NADPH oxidases.[32] Indeed, celastramycin treatment significantly reduced NADPH oxidase activity and Keap1 and upregulated downstream Nrf2 in PAH-PASMCs. Induction of the Nrf2 transcript is an effective approach for enhancing the activity of Nrf2, even though Nrf2 activity is tightly regulated by proteasomal degradation via Keap1-mediated ubiquitination.[54] Nrf2 enables adaptation to oxidants and electrophiles by stimulating the transcriptional activation of about 100 cytoprotective genes, including *GCLC,* which regulates GSH biosynthesis, *HMOX1,* which catalytically degrades potentially toxic heme to biliverdin, and *NQO1,* which inhibits the formation of free radicals via the redox-cycling of quinones. Indeed, in the present study, celastramycin significantly upregulated mRNA levels of *GCLC*, *HMOX1*, and *NQO1* and protein levels of GSH in PAH-PASMCs. Consistently, activation of Nrf2 inhibited PASMC proliferation and ameliorated hypoxia-induced PH in mice.[55] In contrast, celastramycin treatment significantly increased mROS in PAH-PASMCs. This is consistent with the higher levels of ATP production, maximal respiration, and OCR/ECAR ratio in celastramycin-treated cells. Dysregulated mitochondria in PAH-PASMCs show lower mROS production compared with normal PASMCs, and an increase in mROS causes apoptosis in PAH-PASMCs.[56-58] These data indicate that the celastramycin-mediated reduction in ROS (e.g., Nrf2-mediated ROS scavengers, NADPH oxidase-derived ROS reduction) was significant as compared with the celastramycin-mediated increase in mitochondrial ROS production. In total, celastramycin reduced the levels of cytosolic ROS (assessed by DCF and CellROX) through significant upregulation of Nrf2 (ROS scavengers), downregulation of NADPH oxidases, and slight increase in mitochondrial ROS (by increased mitochondrial respiration and ATP production) in PAH-PASMCs.

Celastramycin improves mitochondrial metabolism and networks in PAH-PASMCs.

Celastramycin treatment increased OCR and OCR/ECAR ratio in PAH-PASMCs. The reason why the TCA cycle is upregulated may be that celastramycin reduces PDK1 which inactivates pyruvate dehydrogenase (PDH) to convert pyruvic acid to acetyl CoA. Additionally, celastramycin treatment ameliorated mitochondrial morphology. The mitochondrial network is fragmented in PAH-PASMCs,[29] and this disruption is mechanistically related to imbalanced proliferation and apoptosis in PAH-PASMCs.[29] Fragmentation of the mitochondrial network reflects, in part, increased fission.[43] Fission creates smaller, more discrete mitochondria, which facilitates mitophagy, or accelerates cell proliferation.[59] When mitochondria cannot divide, mitosis does not proceed and cells are arrested in the G2-M phase of the cell cycle.[7] Thus, it is conceivable that celastramycin normalized the balance between fission and fusion in PAH-PASMCs, resulting in increased mitochondrial network activity and decreased proliferation. A possible mechanism of the celastramycin-mediated alteration in this balance may be the downregulation of HIF-1α, which is excessively activated in PAH-PASMCs and is likely an upstream stimulus for impaired mitochondrial fusion and enhanced fission in PAH.[29] Indeed, celastramycin treatment reduced the levels of DRP1, which promotes mitochondrial fission, in PAH-PASMCs. The reason for the celastramycin-mediated downregulation of HIF-1α may involve the suppression of NF-kB signaling. Indeed, NF-κB has been shown to directly affect HIF-1α expression at the HIF-1α promoter region, contributing to the regulation of basal levels of mRNA and protein. Additionally, NF-κB-mediated downstream inflammatory cytokines also have direct effects on mitochondrial function in PAH-PASMCs.[9,16] Furthermore, celastramycin-mediated upregulation of *HMOX1* should lead to altered mitochondrial energy metabolism. Indeed, it has been reported that *HMOX1* in the heart stimulates mitochondrial biogenesis via the induction of Nrf2 and its nuclear translocation. The number of mitochondria is regulated by mitochondrial biogenesis to meet the energy demands of the cell and compensate for cell damage.[59] Thus, celastramycin may have altered the mitochondrial energy metabolism through the progression of mitochondrial biogenesis in PAH-PASMCs. Finally, celastramycin-mediated functional improvement of exercise capacity in the Sugen/hypoxia model indicated that celastramycin directly affects cardiac myocytes in addition to PASMCs in terms of mitochondrial biogenesis. We consider that the celastramycin-mediated metabolic changes may have contributed to the greater effects in Sugen/hypoxia-induced model rather than monocrotaline-induced model.

Study limitations.

There are several limitations of the present study. First, we mainly evaluated ROS levels (cytosolic and mitochondrial), inflammation, and mitochondrial energy metabolism, but there might be other mechanisms through which celastramycin suppresses cell proliferation. Indeed, celastramycin treatment significantly upregulated the eNOS levels, which increase NO production in PAECs. Nrf2 activators are in clinical trial for PH treatment and Nrf2 activation can increase NO and decrease superoxide generation.[60] Thus, it is possible that the mechanism of action of celastramycin is actually via Nrf2-dependent NO upregulation, which could explain both the decreased RVSP and RVH (both via direct effects of NO in cardiomyocytes and also in response to reduced RVSP) rather than an entirely PASMC-mediated effect. Moreover, new approaches for PAH therapy need to show benefit on the top of optimized treatment with currently approved therapy.[20] Thus, the combination of celastramycin with other drug such as sildenafil should be examined in the future. Second, the cytokine data in three animal models are complex and difficult to clearly understand because of the different models with different mechanisms. Third, we were unable to use cardiomyocytes from PAH patients (PAH-CMs) because it is difficult for us to perform primary culture of PAH-CMs.[9] Finally, we selected celastramycin from the 25 analogues, but other analogue might have better effects *in vivo* because some other analogues inhibited cell proliferation more strongly than celastramycin in vitro.

Clinical implications and conclusions.

We found that celastramycin inhibits proliferation of PAH-PASMCs in a dose-dependent manner with small effect on control PASMCs via anti-inflammatory and anti-oxidant effects, accompanied by metabolic improvement. Consistently, celastramycin successfully ameliorated hypoxia-induced PH in mice, monocrotaline-induced PH in rats and Sugen/hypoxia-induced PH in rats. In conclusion, we discovered a new anti-proliferative compound, celastramycin, which is effective in rodent models of PH. Celastramycin could be a promising drug for the treatment of patients with PAH.

ACKNOWLEDGMENTS

We are grateful to the lab members in the Department of Cardiovascular Medicine at Tohoku University for valuable technical assistance, especially Yumi Watanabe, Ai Nishihara, and Hiromi Yamashita, and the assistants of GC-MS analyses at Tohoku Medical Megabank Organization, especially Reina Saijo, and Keiko Umeda.

SOURCES OF FUNDING

This work was supported in part by the grants-in-aid for Scientific Research (15H02535, 15H04816 and 15K15046), all of which are from the Ministry of Education, Culture, Sports, Science and Technology, Tokyo, Japan, the grants-in-aid for Scientific Research from the Ministry of Health, Labour, and Welfare, Tokyo, Japan (10102895), and the grants-in-aid for Scientific Research from the Japan Agency for Medical Research and Development, Tokyo, Japan (15ak0101035h0001, 16ek0109176h0001, 17ek0109227h0001).

DISCLOSURES

None.

REFERENCES

1. Ryan JJ, Archer SL. Emerging concepts in the molecular basis of pulmonary arterial hypertension: part I: metabolic plasticity and mitochondrial dynamics in the pulmonary circulation and right ventricle in pulmonary arterial hypertension. *Circulation*. 2015;131:1691-1702. doi: 10.1161/CIRCULATIONAHA.114.006979.
2. Michelakis ED. Pulmonary arterial hypertension: yesterday, today, tomorrow. *Circ Res*. 2014;115:109-114. doi: 10.1161/CIRCRESAHA.115.301132.
3. Lai YC, Potoka KC, Champion HC, Mora AL, Gladwin MT. Pulmonary arterial hypertension: the clinical syndrome. *Circ Res*. 2014;115:115-130. doi: 10.1161/CIRCRESAHA.115.301146.
4. Montani D, Chaumais MC, Guignabert C, Gunther S, Girerd B, Jais X, Algalarrondo V, Price LC, Savale L, Sitbon O, Simonneau G, Humbert M. Targeted therapies in pulmonary arterial hypertension. *Pharmacol Ther*. 2014;141:172-191. doi: 10.1016/j.pharmthera.2013.10.002.
5. Humbert M, Sitbon O, Chaouat A, Bertocchi M, Habib G, Gressin V, Yaici A, Weitzenblum E, Cordier JF, Chabot F, Dromer C, Pison C, Reynaud-Gaubert M, Haloun A, Laurent M, Hachulla E, Cottin V, Degano B, Jais X, Montani D, Souza R, Simonneau G. Survival in patients with idiopathic, familial, and anorexigen-associated pulmonary arterial hypertension in the modern

management era. *Circulation*. 2010;122:156-163. doi: 10.1161/CIRCULATIONAHA.109.911818.

6. Abe K, Toba M, Alzoubi A, Ito M, Fagan KA, Cool CD, Voelkel NF, McMurtry IF, Oka M. Formation of plexiform lesions in experimental severe pulmonary arterial hypertension. *Circulation*. 2010;121:2747-2754. doi: 10.1161/CIRCULATIONAHA.109.927681.
7. Marsboom G, Toth PT, Ryan JJ, Hong Z, Wu X, Fang YH, Thenappan T, Piao L, Zhang HJ, Pogoriler J, Chen Y, Morrow E, Weir EK, Rehman J, Archer SL. Dynamin-related protein 1-mediated mitochondrial mitotic fission permits hyperproliferation of vascular smooth muscle cells and offers a novel therapeutic target in pulmonary hypertension. *Circ Res*. 2012;110:1484-1497. doi: 10.1161/CIRCRESAHA.111.263848.
8. Bonnet S, Rochefort G, Sutendra G, Archer SL, Haromy A, Webster L, Hashimoto K, Bonnet SN, Michelakis ED. The nuclear factor of activated T cells in pulmonary arterial hypertension can be therapeutically targeted. *Proc Natl Acad Sci U S A*. 2007;104:11418-11423. doi: 10.1073/pnas.0610467104.
9. Paulin R, Michelakis ED. The metabolic theory of pulmonary arterial hypertension. *Circ Res*. 2014;115:148-164. doi: 10.1161/CIRCRESAHA.115.301130.
10. Okada-Iwabu M, Yamauchi T, Iwabu M, Honma T, Hamagami K, Matsuda K, Yamaguchi M, Tanabe H, Kimura-Someya T, Shirouzu M, Ogata H, Tokuyama K, Ueki K, Nagano T, Tanaka A, Yokoyama S, Kadowaki T. A small-molecule AdipoR agonist for type 2 diabetes and short life in obesity. *Nature*. 2013;503:493-499. doi: 10.1038/nature12656.
11. Kikuchi H, Sekiya M, Katou Y, Ueda K, Kabeya T, Kurata S, Oshima Y. Revised structure and synthesis of celastramycin A, a potent innate immune suppressor. *Org Lett*. 2009;16:1693-1695.
12. Yajima M, Takada M, Takahashi N, Kikuchi H, Natori S, Oshima Y, Kurata S. A newly established in vitro culture using transgenic Drosophila reveals functional coupling between the phospholipase A_2-generated fatty acid cascade and lipopolysaccharide-dependent activation of the immune deficiency (IMD) pathway in insect immunity. *Biochem J*. 2003;371:205-210.
13. Tomita T, Ieguchi K, Coin F, Kato Y, Kikuchi H, Oshima Y, Kurata S, Maru Y. ZFC3H1, a zinc finger protein, modulates IL-8 transcription by binding with celastramycin A, a potential immune suppressor. *PLoS One*. 2014;9:e108957. doi: 10.1371/journal.pone.0108957.
14. Vergadi E, Chang MS, Lee C, Liang OD, Liu X, Fernandez-Gonzalez A, Mitsialis SA, Kourembanas S. Early macrophage recruitment and alternative activation are critical for the later development of hypoxia-induced pulmonary hypertension. *Circulation*. 2011;123:1986-1995. doi: 10.1161/CIRCULATIONAHA.110.978627.
15. Fessel JP, West JD. Redox biology in pulmonary arterial hypertension (2013 Grover Conference Series). *Pulm Circ*. 2015;5:599-609. doi: 10.1086/683814.

16. Sutendra G, Dromparis P, Bonnet S, Haromy A, McMurtry MS, Bleackley RC, Michelakis ED. Pyruvate dehydrogenase inhibition by the inflammatory cytokine TNFα contributes to the pathogenesis of pulmonary arterial hypertension. *J Mol Med*. 2011;89:771-783. doi: 10.1007/s00109-011-0762-2).

17. Satoh K, Satoh T, Kikuchi N, Omura J, Kurosawa R, Suzuki K, Sugimura K, Aoki T, Nochioka K, Tatebe S, Miyamichi-Yamamoto S, Miura M, Shimizu T, Ikeda S, Yaoita N, Fukumoto Y, Minami T, Miyata S, Nakamura K, Ito H, Kadomatsu K, Shimokawa H. Basigin mediates pulmonary hypertension by promoting inflammation and vascular smooth muscle cell proliferation. *Circ Res*. 2014;115:738-750. doi: 10.1161/CIRCRESAHA.115.304563.

18. Omura J, Satoh K, Kikuchi N, Satoh T, Kurosawa R, Nogi M, Otsuki T, Kozu K, Numano K, Suzuki K, Sunamura S, Tatebe S, Aoki T, Sugimura K, Miyata S, Hoshikawa Y, Okada Y, Shimokawa H. Protective roles of endothelial AMP-activated protein kinase against hypoxia-induced pulmonary hypertension in mice. *Circ Res*. 2016;119:197-209. doi: 10.1161/CIRCRESAHA.115.308178.

19. Kikuchi N, Satoh K, Kurosawa R, Yaoita N, Elias-Al-Mamun M, Siddique MAH, Omura J, Satoh T, Nogi M, Sunamura S, Miyata S, Saito Y, Hoshikawa Y, Okada Y, Shimokawa H. Selenoprotein P promotes the development of pulmonary arterial hypertension: a possible novel therapeutic target. *Circulation*. 2018;138:600-623. doi: 10.1161/CIRCULATIONAHA.117.033113.

20. Bonnet S, Provencher S, Guignabert C, Perros F, Boucherat O, Schermuly RT, Hassoun PM, Rabinovitch M, Nicolls MR, Humbert M. Translating research into improved patient care in pulmonary arterial hypertension. *Am J Respir Crit Care Med*. 2017;195:583-595. doi: 10.1164/rccm.201607-1515PP.

21. Provencher S, Archer SL, Ramirez FD, Hibbert B, Paulin R, Boucherat O, Lacasse Y, Bonnet S. Standards and methodological rigor in pulmonary arterial hypertension preclinical and translational research. *Circ Res*. 2018;122:1021-1032. doi: 10.1161/CIRCRESAHA.117.312579.

22. Meloche J, Pflieger A, Vaillancourt M, Paulin R, Potus F, Zervopoulos S, Graydon C, Courboulin A, Breuils-Bonnet S, Tremblay E, Couture C, Michelakis ED, Provencher S, Bonnet S. Role for DNA damage signaling in pulmonary arterial hypertension. *Circulation*. 2014;129:786-797. doi: 10.1161/CIRCULATIONAHA.113.006167.

23. Efron B, Tibshirani, Robert. An introduction to the bootstrap. *Chapman and Hall Ltd, London; New York*. 1993

24. Frank Bretz TH, Peter Westfall. Multiple comparisons using R. *Chapman and Hall/CRC*. 2010

25. Shimizu T, Fukumoto Y, Tanaka S, Satoh K, Ikeda S, Shimokawa H. Crucial role of ROCK2 in vascular smooth muscle cells for hypoxia-induced pulmonary hypertension in mice. *Arterioscler*

Thromb Vasc Biol. 2013;33:2780-2791. doi: 10.1161/ATVBAHA.113.301357.

26. Dabral S, Tian X, Kojonazarov B, Savai R, Ghofrani HA, Weissmann N, Florio M, Sun J, Jonigk D, Maegel L, Grimminger F, Seeger W, Savai Pullamsetti S, Schermuly RT. Notch1 signalling regulates endothelial proliferation and apoptosis in pulmonary arterial hypertension. *Eur Respir J*. 2016;48:1137-1149. doi: 10.1183/13993003.00773-2015.

27. Sunamura S, Satoh K, Kurosawa R, Ohtsuki T, Kikuchi N, Elias-Al-Mamun M, Shimizu T, Ikeda S, Suzuki K, Satoh T, Omura J, Nogi M, Numano K, Siddique MAH, Miyata S, Miura M, Shimokawa H. Different roles of myocardial ROCK1 and ROCK2 in cardiac dysfunction and postcapillary pulmonary hypertension in mice. *Proc Natl Acad Sci U S A*. 2018;115:E7129-E7138. doi: 10.1073/pnas.1721298115.

28. Nogi M, Satoh K, Sunamura S, Kikuchi N, Satoh T, Kurosawa R, Omura J, Al-Mamun ME, Siddique MAH, Numano K, Kudo S, Miyata S, Akiyama M, Kumagai K, Kawamoto S, Saiki Y, Shimokawa H. SmgGDS prevents thoracic aortic aneurysm formation and rupture by phenotypic preservation of aortic smooth muscle cells. *Circulation*. 2018;138:2413-2433. doi: 10.1161/CIRCULATIONAHA.118.035648.

29. Bonnet S, Michelakis ED, Porter CJ, Andrade-Navarro MA, Thebaud B, Bonnet S, Haromy A, Harry G, Moudgil R, McMurtry MS, Weir EK, Archer SL. An abnormal mitochondrial-hypoxia inducible factor-1α-Kv channel pathway disrupts oxygen sensing and triggers pulmonary arterial hypertension in fawn hooded rats: similarities to human pulmonary arterial hypertension. *Circulation*. 2006;113:2630-2641. doi: 10.1161/CIRCULATIONAHA.105.609008.

30. Papaiahgari S, Kleeberger SR, Cho HY, Kalvakolanu DV, Reddy SP. NADPH oxidase and ERK signaling regulates hyperoxia-induced Nrf2-ARE transcriptional response in pulmonary epithelial cells. *J Biol Chem*. 2004;279:42302-42312. doi: 10.1074/jbc.M408275200.

31. Brewer AC, Murray TV, Arno M, Zhang M, Anilkumar NP, Mann GE, Shah AM. Nox4 regulates Nrf2 and glutathione redox in cardiomyocytes in vivo. *Free Radic Biol Med*. 2011;51:205-215. doi: 10.1016/j.freeradbiomed.2011.04.022.

32. Kovac S, Angelova PR, Holmstrom KM, Zhang Y, Dinkova-Kostova AT, Abramov AY. Nrf2 regulates ROS production by mitochondria and NADPH oxidase. *Biochim Biophys Acta*. 2015;1850:794-801. doi: 10.1016/j.bbagen.2014.11.021.

33. Sutendra G, Michelakis ED. The metabolic basis of pulmonary arterial hypertension. *Cell Metab*. 2014;19:558-573. doi: 10.1016/j.cmet.2014.01.004.

34. Rhodes CJ, Ghataorhe P, Wharton J, Rue-Albrecht KC, Hadinnapola C, Watson G, Bleda M, Haimel M, Coghlan G, Corris PA, Howard LS, Kiely DG, Peacock AJ, Pepke-Zaba J, Toshner MR, Wort SJ, Gibbs JS, Lawrie A, Graf S, Morrell NW, Wilkins MR. Plasma metabolomics implicates

modified transfer RNAs and altered bioenergetics in the outcomes of pulmonary arterial hypertension. *Circulation*. 2017;135:460-475. doi: 10.1161/CIRCULATIONAHA.116.024602.

35. Ogawa A, Firth AL, Yao W, Rubin LJ, Yuan JX. Prednisolone inhibits PDGF-induced nuclear translocation of NF-κB in human pulmonary artery smooth muscle cells. *Am J Physiol Lung Cell Mol Physiol*. 2008;295:L648-657. doi: 10.1152/ajplung.90245.2008.
36. Meloche J, Potus F, Vaillancourt M, Bourgeois A, Johnson I, Deschamps L, Chabot S, Ruffenach G, Henry S, Breuils-Bonnet S, Tremblay E, Nadeau V, Lambert C, Paradis R, Provencher S, Bonnet S. Bromodomain-containing protein 4: the epigenetic origin of pulmonary arterial hypertension. *Circ Res*. 2015;117:525-535. doi: 10.1161/CIRCRESAHA.115.307004.
37. Hussong M, Borno ST, Kerick M, Wunderlich A, Franz A, Sultmann H, Timmermann B, Lehrach H, Hirsch-Kauffmann M, Schweiger MR. The bromodomain protein BRD4 regulates the Keap1/Nrf2-dependent oxidative stress response. *Cell Death Dis*. 2014;5:e1195. doi: 10.1038/cddis.2014.157.
38. Michaeloudes C, Mercado N, Clarke C, Bhavsar PK, Adcock IM, Barnes PJ, Chung KF. Bromodomain and extraterminal proteins suppress NF-E2-related factor 2-mediated antioxidant gene expression. *J Immunol*. 2014;192:4913-4920. doi: 10.4049/jimmunol.1301984.
39. Ranchoux B, Meloche J, Paulin R, Boucherat O, Provencher S, Bonnet S. DNA damage and pulmonary hypertension. *Int J Mol Sci*. 2016;17:pii: E990. doi: 10.3390/ijms17060990.
40. Meola N, Domanski M, Karadoulama E, Chen Y, Gentil C, Pultz D, Vitting-Seerup K, Lykke-Andersen S, Andersen JS, Sandelin A, Jensen TH. Identification of a nuclear exosome decay pathway for processed transcripts. *Mol Cell*. 2016;64:520-533. doi: 10.1016/j.molcel.2016.09.025.
41. Lee NN, Chalamcharla VR, Reyes-Turcu F, Mehta S, Zofall M, Balachandran V, Dhakshnamoorthy J, Taneja N, Yamanaka S, Zhou M, Grewal SI. Mtr4-like protein coordinates nuclear RNA processing for heterochromatin assembly and for telomere maintenance. *Cell*. 2013;155:1061-1074. doi: 10.1016/j.cell.2013.10.027.
42. Chlebowski A, Lubas M, Jensen TH, Dziembowski A. RNA decay machines: the exosome. *Biochim Biophys Acta*. 2013;1829:552-560. doi: 10.1016/j.bbagrm.2013.01.006.
43. Ryan JJ, Marsboom G, Fang YH, Toth PT, Morrow E, Luo N, Piao L, Hong Z, Ericson K, Zhang HJ, Han M, Haney CR, Chen CT, Sharp WW, Archer SL. PGC1α-mediated mitofusin-2 deficiency in female rats and humans with pulmonary arterial hypertension. *Am J Respir Crit Care Med*. 2013;187:865-878. doi: 10.1164/rccm.201209-1687OC.
44. Fernandez-Marcos PJ, Auwerx J. Regulation of PGC-1α, a nodal regulator of mitochondrial biogenesis. *Am J Clin Nutr*. 2011;93:884S-890. doi: 10.3945/ajcn.110.001917.
45. Wan Z, Root-McCaig J, Castellani L, Kemp BE, Steinberg GR, Wright DC. Evidence for the role

of AMPK in regulating PGC-1 α expression and mitochondrial proteins in mouse epididymal adipose tissue. *Obesity (Silver Spring)*. 2014;22:730-738. doi: 10.1002/oby.20605.

46. Rabinovitch RC, Samborska B, Faubert B, Ma EH, Gravel SP, Andrzejewski S, Raissi TC, Pause A, St-Pierre J, Jones RG. AMPK maintains cellular metabolic homeostasis through regulation of mitochondrial reactive oxygen species. *Cell Rep*. 2017;21:1-9. doi: 10.1016/j.celrep.2017.09.026.
47. Bonnet S, Paulin R, Boucherat O. Small SeP or giant leap for pulmonary hypertension research? *Circulation*. 2018;138:624-626. doi: 10.1161/CIRCULATIONAHA.118.035427.
48. Kikuchi N, Satoh K, Saito Y, Shimokawa H. Response by Kikuchi et al regarding article, "selenoprotein P promotes the development of pulmonary arterial hypertension: a possible novel therapeutic target". *Circulation*. 2018;139:724-725. doi: 10.1161/CIRCULATIONAHA.117.033113.
49. Pullen C, Schmitz P, Meurer K, Bamberg DD, Lohmann S, De Castro Franca S, Groth I, Schlegel B, Mollmann U, Gollmick F, Grafe U, Leistner E. New and bioactive compounds from Streptomyces strains residing in the wood of Celastraceae. *Planta*. 2002;216:162-167. doi: 10.1007/s00425-002-0874-6.
50. Voelkel NF, Tuder RM, Bridges J, Arend WP. Interleukin-1 receptor antagonist treatment reduces pulmonary hypertension generated in rats by monocrotaline. *Am J Respir Cell Mol Biol*. 1994;11:664-675.
51. Hashimoto-Kataoka T, Hosen N, Sonobe T, Arita Y, Yasui T, Masaki T, Minami M, Inagaki T, Miyagawa S, Sawa Y, Murakami M, Kumanogoh A, Yamauchi-Takihara K, Okumura M, Kishimoto T, Komuro I, Shirai M, Sakata Y, Nakaoka Y. Interleukin-6/interleukin-21 signaling axis is critical in the pathogenesis of pulmonary arterial hypertension. *Proc Natl Acad Sci U S A*. 2015. doi: 10.1073/pnas.1424774112.
52. Bauer EM, Chanthaphavong RS, Sodhi CP, Hackam DJ, Billiar TR, Bauer PM. Genetic deletion of toll-like receptor 4 on platelets attenuates experimental pulmonary hypertension. *Circ Res*. 2014;114:1596-1600. doi: 10.1161/CIRCRESAHA.114.303662.
53. Chen C-Y, Gherzi R, Ong S-E, Chan EL, Raijmakers R, Pruijn GJM, Stoecklin G, Moroni C, Mann M, Karin M. AU binding proteins recruit the exosome to degrade ARE-containing mRNAs. *Cell*. 2001;107:451-464
54. Suzuki T, Shibata T, Takaya K, Shiraishi K, Kohno T, Kunitoh H, Tsuta K, Furuta K, Goto K, Hosoda F, Sakamoto H, Motohashi H, Yamamoto M. Regulatory nexus of synthesis and degradation deciphers cellular Nrf2 expression levels. *Mol Cell Biol*. 2013;33:2402-2412
55. Eba S, Hoshikawa Y, Moriguchi T, Mitsuishi Y, Satoh H, Ishida K, Watanabe T, Shimizu T, Shimokawa H, Okada Y, Yamamoto M, Kondo T. The nuclear factor erythroid 2-related factor 2

activator oltipraz attenuates chronic hypoxia-induced cardiopulmonary alterations in mice. *Am J Respir Cell Mol Biol*. 2013;49:324-333. doi: 10.1165/rcmb.2011-0396OC.

56. Sutendra G, Michelakis ED. Pulmonary arterial hypertension: challenges in translational research and a vision for change. *Sci Transl Med*. 2013;5:208sr205

57. Paulin R, Dromparis P, Sutendra G, Gurtu V, Zervopoulos S, Bowers L, Haromy A, Webster L, Provencher S, Bonnet S, Michelakis ED. Sirtuin 3 deficiency is associated with inhibited mitochondrial function and pulmonary arterial hypertension in rodents and humans. *Cell Metab*. 2014;20:827-839. doi: 10.1016/j.cmet.2014.08.011.

58. Bonnet S, Archer SL, Allalunis-Turner J, Haromy A, Beaulieu C, Thompson R, Lee CT, Lopaschuk GD, Puttagunta L, Bonnet S, Harry G, Hashimoto K, Porter CJ, Andrade MA, Thebaud B, Michelakis ED. A mitochondria-K^+ channel axis is suppressed in cancer and its normalization promotes apoptosis and inhibits cancer growth. *Cancer Cell*. 2007;11:37-51. doi: 10.1016/j.ccr.2006.10.020.

59. Archer SL. Mitochondrial dynamics--mitochondrial fission and fusion in human diseases. *N Engl J Med*. 2013;369:2236-2251. doi: 10.1056/NEJMra1215233.

60. Hu J, Xu Q, McTiernan C, Lai YC, Osei-Hwedieh D, Gladwin M. Novel Targets of Drug Treatment for Pulmonary Hypertension. *Am J Cardiovasc Drugs*. 2015;15:225-234. doi: 10.1007/s40256-015-0125-4.

FIGURE LEGENDS

Figure 1. Screening of a Novel Compound that Inhibits PAH-PASMC Proliferation

(**A**) The schema of the primary culture of pulmonary artery smooth muscle cells from patients with pulmonary arterial hypertension (PAH-PASMCs) and screening of the Tohoku University Compound Library (5,562 compounds). MTT, 3-(4,5-di-methylthiazol-2-yl)-2,5- diphenyltetrazolium bromide. (**B**) Schematic outline of high-throughput screening to identify celastramycin that inhibit PAH-PASMC proliferation with minimal harmful effects. (**C**) Results of the first screening of 5,562 compounds. The ratio of assay units by MTT assay after treatment with 5,562 compounds (5 μmol/L) or vehicle for 24 hours compared with day 0. Blue represents the MTT levels of PAH-PASMCs after treatment with 5,562 compounds and we selected 80 compounds in the yellow square. (**D**) Results of the second screening of 80 compounds. The ratio of assay units by MTT assay of PAH-PASMCs or PASMCs from healthy donors (control PASMCs) after treatment with 80 compounds (5 μmol/L) or vehicle for 48 hours compared with day 0. Blue represents the MTT levels of PAH-PASMCs and green represents control PASMCs after treatment with 80 compounds and we selected celastramycin in the yellow square. (**E**) Results of concentration-dependent assays with 9 compounds in PAH-PASMCs and control PASMCs. The ratio of assay units by MTT assay after treatment with different concentrations (0, 0.1, 1, and 5 μmol/L) of 9 compounds for 48 hours as compared with day 0 (n=8 each). The 9 compounds are Celastramycin, Maleimide, Gitoxigenin, Puromycin, Emetine, $C_6H_3IN_2O_4$, 1,4-Naphtoquinone, $C_{22}H_{33}C_{l2}N_7O_6$, and $C_{11}H_{14}N_2O_3$. (**F**) RealTime-Glo assay, in which cell viability was measured intermittently after treatment with different concentrations (0, 0.1, 1, 5, and 10 μmol/L) of celastramycin (n=8 each). (**G**) Results of concentration-dependent apoptotic assays stained for Annexin V and TUNEL in PAH-PASMCs after treatment with vehicle or celastramycin (CEL) for 48 hours (20 images/group). Scale bars, 50 μm. Data represent the mean±SEM. *P<0.05. Comparisons of parameters were performed with one-way ANOVA followed by Dunnett's test for multiple comparisons.

Figure 2. Celastramycin Analogues and Structure-activity Correlation

(**A**) The chemical structures of eight analogues, a-h, with different lengths of alkyl chain (R). (**B**) The ratio of cell numbers after treatment with 25 analogues for 48 hours compared with day 0 (1 μmol/L, n=8 each). Cell numbers were measured by MTT, 3-(4,5-di-methylthiazol-2-yl)- 2,5-diphenyltetrazolium bromide assay. (**C**) Structure-activity correlation between the length of the alkyl chain (R) and proliferation of pulmonary artery smooth muscle cells from patients with pulmonary arterial hypertension (PAH-PASMCs). (**D**) The chemical structure of one analogue, i, which substituted R into a chlorine atom. (**E**) The chemical structures of five analogues, j-n, in which one or two branches in the basal common structure "e" were

modified. (**F**) The chemical structures of 11 analogues, o-y, in which the basal common structure "e" were excessively modified. (**G**) The levels of reactive oxygen species (ROS) in PAH-PASMCs assessed by CellROX after treatment with the 25 analogues for 24 hours (*n*=3 each). Data represent the mean±SEM. **P*<0.05. Comparisons of parameters were performed with an unpaired Student's *t*-test or Dunnett's test for multiple comparisons. Linear associations between two continuous variables were analyzed using a linear regression model.

Figure 3. Celastramycin-mediated Recovery of Mitochondrial Functions in PAH-PASMCs

(**A**) RT-PCR analysis of HIF-1α (*HIF1A*) mRNA in control PASMCs and PAH-PASMCs after the treatment with celastramycin or the control vehicle for 24 hours (*n*=6) and quantification of hypoxia-inducible factor-1α (HIF-1α), pyruvate dehydrogenase lipoamide kinase isozyme 1 (PDK1) and dynamin-1-like protein (DRP1) in control PASMCs and PAH-PASMCs after the treatment with celastramycin or the control vehicle for 24 hours (*n*=6). (**B**) Quantification of Kelch-like ECH-associated protein 1 (Keap1) in total cell lysate and NF-E2-related factor 2 (Nrf2) in nuclear extract of control PASMCs and PAH-PASMCs after the treatment with celastramycin or vehicle for 24 hours (*n*=6). (**C**) RT-PCR analysis of Nrf2 (*NFE2L2*) mRNA in control PASMCs and PAH-PASMCs after the treatment with celastramycin or the control vehicle for 24 hours (*n*=6). (**D**) Left, representative images of CellROX Deep Red fluorescence in control PASMCs and PAH-PASMCs. Nuclei were counter-stained using DAPI. Scale bars, 50 μm. Right, quantification of CellROX and DCF fluorescence intensity in control PASMCs and PAH-PASMCs after the treatment with celastramycin or control vehicle for 24 hours (*n*=8 each). (**E**) Quantification of NADPH oxidase activity in control PASMCs and PAH-PASMCs after the treatment with celastramycin or the control vehicle for 12 hours (*n*=8 each). (**F**) Quantification of GSH/GSSG ratio in control PASMCs and PAH-PASMCs after vehicle or celastramycin treatment for 4 hours (*n*=8 each). GSH, glutathione; GSSG, oxidized glutathione. (**G**) Quantification of mitochondrial ROS assessed by MitoSOX fluorescence intensity in control PASMCs and PAH-PASMCs after the treatment with celastramycin or the control vehicle for 24 hours (*n*=8 each). (**H**) Quantification of the mitochondrial oxygen consumption rate (OCR) of control PASMCs and PAH-PASMCs after the treatment with celastramycin or the control vehicle for 24 hours (*n*=5). (**I**) Quantification of the OCR of control PASMCs and PAH-PASMCs after the treatment with celastramycin or the control vehicle for 24 hours (*n*=5 each). Oligomycin inhibits adenosine triphosphate (ATP) synthase (complex V) and the decrease in OCR followed by oligomycin correlates to the mitochondrial respiration associated with cellular ATP production. Carbonyl cyanide-4 (trifluoromethoxy) phenylhydrazone (FCCP) is an uncoupling agent that disrupts the mitochondrial membrane potential. As a result, electron flow through the electron transport chain (ETC) is uninhibited and oxygen is maximally consumed by complex IV. Rotenone and antimycin A were injected to inhibit the flux of electrons through

complex I and III, respectively, and thus shut down mitochondrial oxygen consumption. (**J**) Left, representative images of control PASMCs and PAH-PASMCs labeled for mitochondria after the treatment with celastramycin or the control vehicle for 24 hours. Nuclei were counter-stained using DAPI. Scale bars, 20 μm. Right, quantification of mitochondrial fragmentation in control PASMCs and PAH-PASMCs labeled for mitochondria after the treatment with celastramycin or the control vehicle for 24 hours. (**K**) Representative transmission electron microscopy (TEM) images of control PASMCs and PAH-PASMCs after the treatment with celastramycin or the control vehicle for 24 hours. Scale bars, 2 μm. Data represent the mean±SEM. **P*<0.05. Comparisons of parameters were performed with two-way ANOVA, followed by Tukey's HSD test for multiple comparisons.

Figure 4. Celastramycin-mediated Inhibition of PAH-PASMC Proliferation

(**A**) The ratio of cell numbers in pulmonary artery smooth muscle cells from patients with pulmonary arterial hypertension (PAH-PASMCs) treated with control siRNA (si-Ctrl) or si-NF-κB for 48 hours (*n*=8 each). Cell numbers were measured by 3-(4,5-di-methylthiazol-2-yl)-2,5-diphenyltetrazolium bromide assay. (**B**) Quantification of NF-κB in nuclear extracts of control PASMCs and PAH-PASMCs after the treatment with celastramycin or the control vehicle for 24 hours (*n*=6). (**C**) Quantification of phosphorylated ERK1/2 and total ERK1/2 in total cell lysates of control PASMCs and PAH-PASMCs after the treatment with celastramycin or the control vehicle for 24 hours (*n*=6). (**D**) RT-PCR of NF-κB p65 (*RELA*) and toll-like receptor 4 (*TLR4)* mRNA in control PASMCs and PAH-PASMCs after the treatment with celastramycin or the control vehicle for 24 hours (*n*=6). (**E**) Quantification of bromodomain-containing protein4 (BRD4) and survivin in total cell lysate and nuclear factor of activated T calls 2 (NFATc2) in nuclear extract of control PASMCs of PAH-PASMCs after the treatment with celastramycin or vehicle for 24 hours (*n*=6). (**F**) RT-PCR analysis of Keap1 (*KEAP1*) mRNA in PAH-PASMCs after treatment with si-BRD4 or si-control for 48 hours (*n*=6). (**G**) Schematic representation of the molecular mechanisms promoting inflammation, oxidative stress, and mitochondrial dysfunction through activation of hypoxia inducible factor 1α (HIF-1α) and NF-κB in PAH-PASMCs. Constitutively activated HIF-1α induces the transcription of many genes and dysregulation of mitochondrial energy metabolism, which promotes cell proliferation, apoptosis-resistance, survival, and stress resistance by targeting several downstream genes. Celastramycin treatment downregulates HIF-1α and NF-κB and upregulates Nrf2 in PAH-PASMCs. These effects result in decreased reactive oxygen species (ROS) and inflammation with recovered mitochondrial energy metabolism, leading to inhibition of excessive proliferation in PAH-PASMCs. Data represent the mean±SEM. **P*<0.05. Comparisons of parameters were performed with two-way ANOVA, followed by Tukey's HSD test for multiple comparisons.

Figure 5. ZFC3H1-mediated Inhibition of BRD4 and HIF-1α by Celastramycin Treatment

(**A**) RT-PCR analysis and Western blotting of BRD4 in PAH-PASMCs after treatment with si-ZFC3H1 or si-control for 48 hours (*n*=6). (**B**) RT-PCR analysis of HIF-1α (*HIF1A*) and dynamin-1-like protein (*DNM1L*) mRNA in pulmonary artery smooth muscle cells from patients with pulmonary arterial hypertension (PAH-PASMCs) after treatment with si-ZFC3H1 or si-control for 48 hours (*n*=6). (**C**) RT-PCR analysis of Keap1 (*KEAP1*), Nrf2 (*NFE2L2*), and SOD2 (*SOD2*) mRNA in PAH-PASMCs after treatment with si-ZFC3H1 or si-control for 48 hours (*n*=6). (**D**) RT-PCR analysis and Western blotting of BRD4 in PAH-PASMCs after the treatment with *ZFC3H1* plasmid DNA or control plasmid DNA for 48 hours (*n*=6). (**E**) RT-PCR analysis of HIF-1α (*HIF1A*) and dynamin-1-like protein (*DNM1L*) mRNA in pulmonary artery smooth muscle cells from patients with pulmonary arterial hypertension (PAH-PASMCs) after the treatment with *ZFC3H1* plasmid DNA or control plasmid DNA for 48 hours (*n*=6). (**F**) RT-PCR analysis of Keap1 (*KEAP1*), Nrf2 (*NFE2L2*) and SOD2 (*SOD2*) mRNA in PAH-PASMCs after the treatment with *ZFC3H1* plasmid DNA or control plasmid DNA for 48 hours (*n*=6). (**G**) Schematic representation of the molecular mechanisms of celastramycin-mediated effects on pulmonary artery smooth muscle cells from patients with pulmonary arterial hypertension (PAH-PASMCs). Abnormally activated hypoxia-inducible factor-1α (HIF-1α) and nuclear factor-κB (NF-κB) promotes inflammation, oxidative stress, and mitochondrial dysfunction, which induce excessive proliferation of PAH-PASMCs. Activation of NF-κB also increases production of cytokines/chemokines and growth factors, which recruit abundant inflammatory cells, leading to additional production of growth factors. Secreted growth factors activate NADPH oxidases (NOX), one of the main sources of intracellular ROS, and induce production of cytosolic reactive oxygen species (ROS) in PAH-PASMCs. Here, celastramycin directly binds to zinc finger C3H1 domain-containing protein (ZFC3H1), a zinc finger protein, which downregulates the expression of bromodomain-containing protein 4 (BRD4) and HIF-1α. Celastramycin-mediated decrease in BRD4 downregulates NF-κB and Kelch-like ECH-associated protein 1 (Keap1), which suppress inflammation and activate NF-E2-related factor 2 (Nrf2), leading to upregulation of antioxidants, such as NAD(P)H quinone dehydrogenase-1 (*NQO1*), superoxide dismutase 2 (*SOD2*), heme oxygenase-1 (*HMOX1*), and glutamate-cysteine ligase catalytic subunit (*GCLC*), resulting in inhibition of ROS production. Constitutively activated HIF-1α in PAH-PASMCs upregulates dynamin-1-like protein (DRP1) and promotes mitochondrial fission and induces dysregulation of mitochondrial energy metabolism, leading to less oxidative phosphorylation (OXPHOS) with metabolic abnormality. Mitochondrial ROS (mROS) promotes phosphorylation of AMP-activated protein kinase (AMPK) that induces peroxisome proliferator-activated receptor γ coactivator 1-α (PGC-1α) to promote mitochondrial biogenesis, whereas mROS is downregulated because of mitochondrial metabolic abnormality in PAH-PASMCs. These mitochondrial abnormalities are reversed by ZFC3H1-mediated HIF-1α downregulation. Altogether, celastramycin inhibited abnormal proliferation of PAH-

PASCMs through changes in these transcription factors. Data represent the mean±SEM. *P<0.05. Comparisons of parameters were performed with an unpaired Student's t-test.

Figure 6. Celastramycin Ameliorates Hypoxia-induced Pulmonary Hypertension in Mice

(**A**) Schematic protocols for celastramycin administration to hypoxia-induced pulmonary hypertension (PH) in wild-type mice, in which 10 mg/kg/day celastramycin or control vehicle was administered using an osmotic pump during the 3 weeks of hypoxic exposure (10% O_2). (**B**) The time-course of body weight from the starting point of administration of celastramycin or control vehicle under normoxia (21% O_2, n=8 each) or hypoxia (10% O_2, n=14 each) for 3 weeks. (**C**) Systolic blood pressure of hypoxia-induced PH mice and control mice measured by tail cuff systems after the treatment with celastramycin or control vehicle for 3 weeks (n=6 each). (**D**) Levels of cytokines/chemokines and growth factors in the lungs after the treatment with celastramycin or vehicle under normoxia or hypoxia (10% O_2) for 3 weeks (n=6 each). (**E**) Muscularization of the distal pulmonary arteries with a diameter of 20–70 μm after the treatment with celastramycin or control vehicle under normoxia (n=8 each) or hypoxia (n=14 each). N, non-muscularized vessels; P, partially muscularized vessels; F, fully muscularized vessels. Scale bar, 25 μm. (**F**) Right ventricular systolic pressure (RVSP) and right ventricular hypertrophy (RVH) in wild-type mice after the treatment with celastramycin or control vehicle under normoxia (n=8 each) or hypoxia (10% O_2, n=14 each) for 3 weeks. RVH, the ratio of the right ventricle to the left ventricle plus septum (RV/LV+S). Data represent the mean±SEM. *P<0.05. Comparisons of means between 2 groups by the bootstrap method. The multiplicity of the testing was adjusted by the Holm's method.

Figure 7. Celastramycin Ameliorates Monocrotaline-induced Pulmonary Hypertension in Rats

(**A**) Schematic protocols for celastramycin administration to monocrotaline (MCT)-induced pulmonary hypertension (PH) in rats, in which 3 mg/kg/day celastramycin was administered (intraperitoneal injection) for 3 weeks after MCT injection (60 mg/kg, subcutaneous injection). (**B**) The time-course of body weight changes from the starting point of administration of celastramycin or control vehicle for 3 weeks (n=14). (**C**) Levels of cytokines/chemokines and growth factors in the lungs of monocrotaline-induced pulmonary hypertension in rats and control rats after the treatment with celastramycin or control vehicle for 3 weeks (n=6 each). (**D**) Medial wall thickness (MWT) of the distal pulmonary arteries in rats (control, n=7; celastramycin and vehicle, n=11 each). Scale bar, 50 μm. (**E**) Right ventricular systolic pressure (RVSP, left) and right ventricular hypertrophy (RVH) in rats (control, n=7; celastramycin and vehicle, n=11 each). RVH, the ratio of the right ventricle to the left ventricle plus septum (RV/LV+S). Data represent the mean±SEM. *P<0.05. Comparisons of means between 2 groups by the bootstrap method. The multiplicity of the testing was adjusted by the Holm's method.

Figure 8. Celastramycin Ameliorates Sugen/hypoxia-induced Pulmonary Hypertension in Rats

(**A**) Schematic protocols for celastramycin administration to the Sugen/hypoxia rat model, in which rats were exposed to chronic hypoxia (10% O_2) for 3 weeks in combination with the VEGF receptor blocker SU5416 (20 mg/kg, subcutaneous injection) followed by daily administration of 3 mg/kg body weight celastramycin or control vehicle by intraperitoneal injection for 2 weeks. (**B**) The time-course of body weight changes from the starting point of SU5416 injection for 5 weeks in Sugen/hypoxia rats and control rats (*n*=12 each). (**C**) Levels of interleukin (IL)-2 and IL-6 in the lungs of Sugen/hypoxia rats and control rats after the treatment with celastramycin or control vehicle for 2 weeks (*n*=6 each). (**D**) Left, representative pictures of distal pulmonary arteries. Middle, muscularization of the distal pulmonary arteries with a diameter of 50–100 μm after the treatment with celastramycin or vehicle control in rats (*n*=12 each). N, non-muscularized vessels; P, partially muscularized vessels; F, fully muscularized vessels. Right, medial wall thickness (MWT) of the distal pulmonary arteries in rats (*n*=12 each). Scale bar, 50 μm. (**E**) Right ventricular systolic pressure (RVSP) and right ventricular hypertrophy (RVH) (*n*=12 each). RVH, the ratio of the right ventricle to the left ventricle plus septum (RV/LV+S). (**F**) Left, representative echocardiographic images illustrating RV diastolic diameter (RVDd), RV fractional area change (RVFAC), PA acceleration time (PAAT), and tricuspid annular plane systolic excursion (TAPSE). Right, echocardiographic measurement of RVDd, RVFAC, PAAT, TAPSE, and cardiac output (CO) (*n*=12 each). (**G**) Echocardiographic measurement of LV diastolic diameter (LVDd) and LV ejection fraction (LVEF) (*n*=12 each). (**H**) Mean pulmonary artery pressure (mPAP) and total pulmonary resistance (TPR) in rats (*n*=12 each). (**I**) Walking distance assessed by treadmill test (*n*=12 each). Data represent the mean±SEM. **P*<0.05. Comparisons of means between 2 groups by the bootstrap method. The multiplicity of the testing was adjusted by the Holm's method.

NOVELTY AND SIGNIFICANCE

What Is Known?

- Pulmonary arterial smooth muscle cells (PASMCs) from patients with pulmonary arterial hypertension (PAH) rigorously proliferate like cancer cells and finally occlude the distal pulmonary arteries, which is associated with increased production of inflammatory factors and adaptation of mitochondrial metabolism to a hyperproliferative state.

- Celastramycin is a benzoyl pyrrole-type compound originally found in a bacterial extract which suppresses NF-κB-like transcriptional factors.

What New Information Does This Article Contribute?

- Celastramycin inhibits cell proliferation of PASMCs from patients with PAH dose-dependently with small effects on control PASMCs. Celastramycin also inhibits inflammation and reactive oxygen species and recovers mitochondrial energy metabolism.

- Treatment with celastramycin ameliorates pulmonary hypertension in rodent models.

- Celastramycin is a promising drug for the treatment of patients with PAH that targets anti-proliferative effects on PAH-PASMCs.

To our knowledge, this is the first study demonstrating that celastramycin inhibits cell proliferation of PASMCs from patients with PAH and ameliorates pulmonary hypertension in rodent models. We screened 5,562 compounds from an original library using high-throughput screening and found celastramycin as a promising drug for PAH. Mechanistic analysis demonstrated that celastramycin reduces excessive proliferation of PASMCs from patients with PAH with changes in hypoxia-inducible factor 1α, nuclear factor-κB, and NF-E2-related factor 2, leading to less inflammation and reduced ROS levels and recovered mitochondrial energy metabolism. Furthermore, we showed that these celastramycin-mediated effects are regulated by the zinc finger C3H1 domain-containing protein, a binding partner of celastramycin. Thus, the findings set the stage for further investigating the use of celastramycin for treatment of patients with PAH.

Figure 1

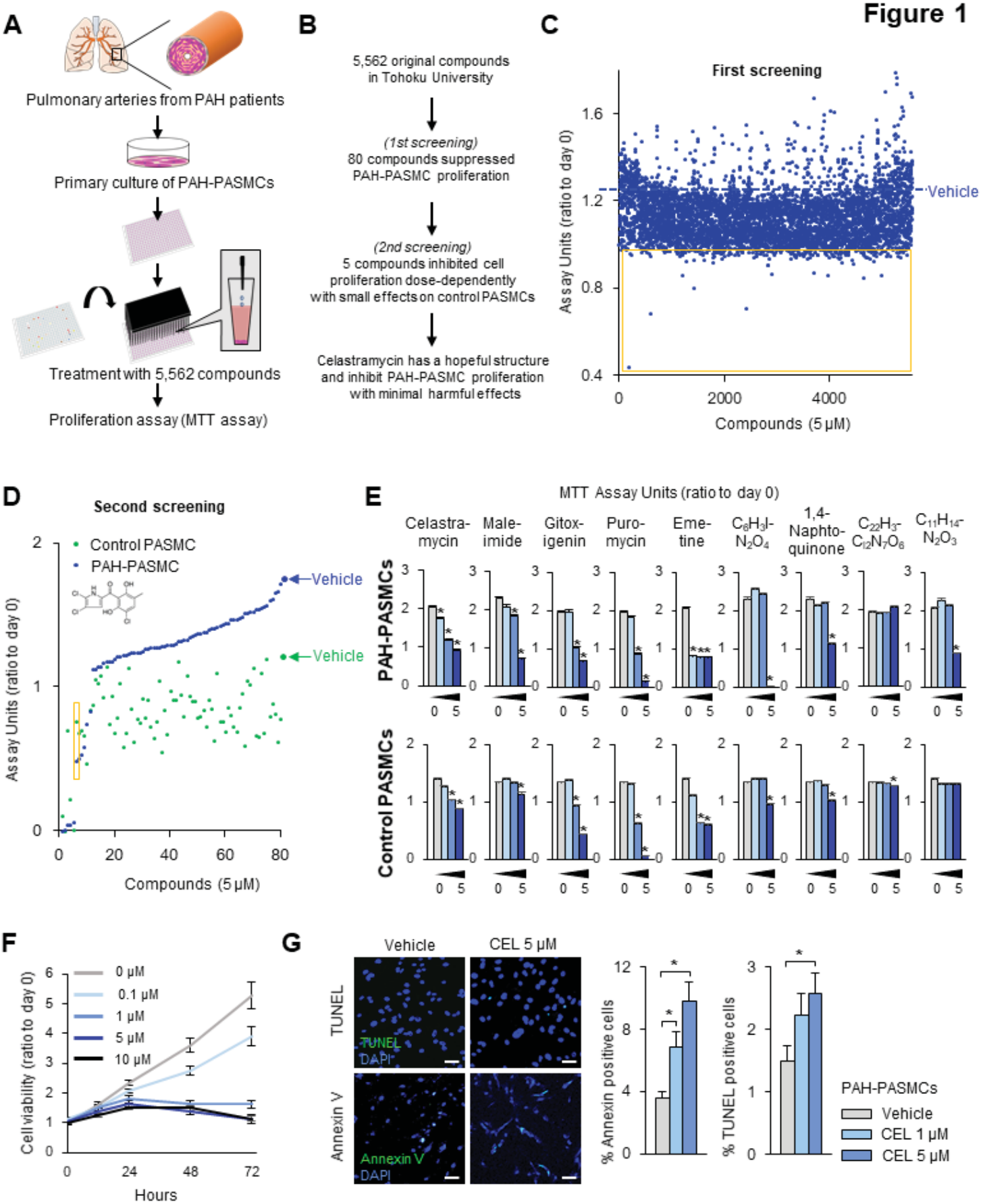

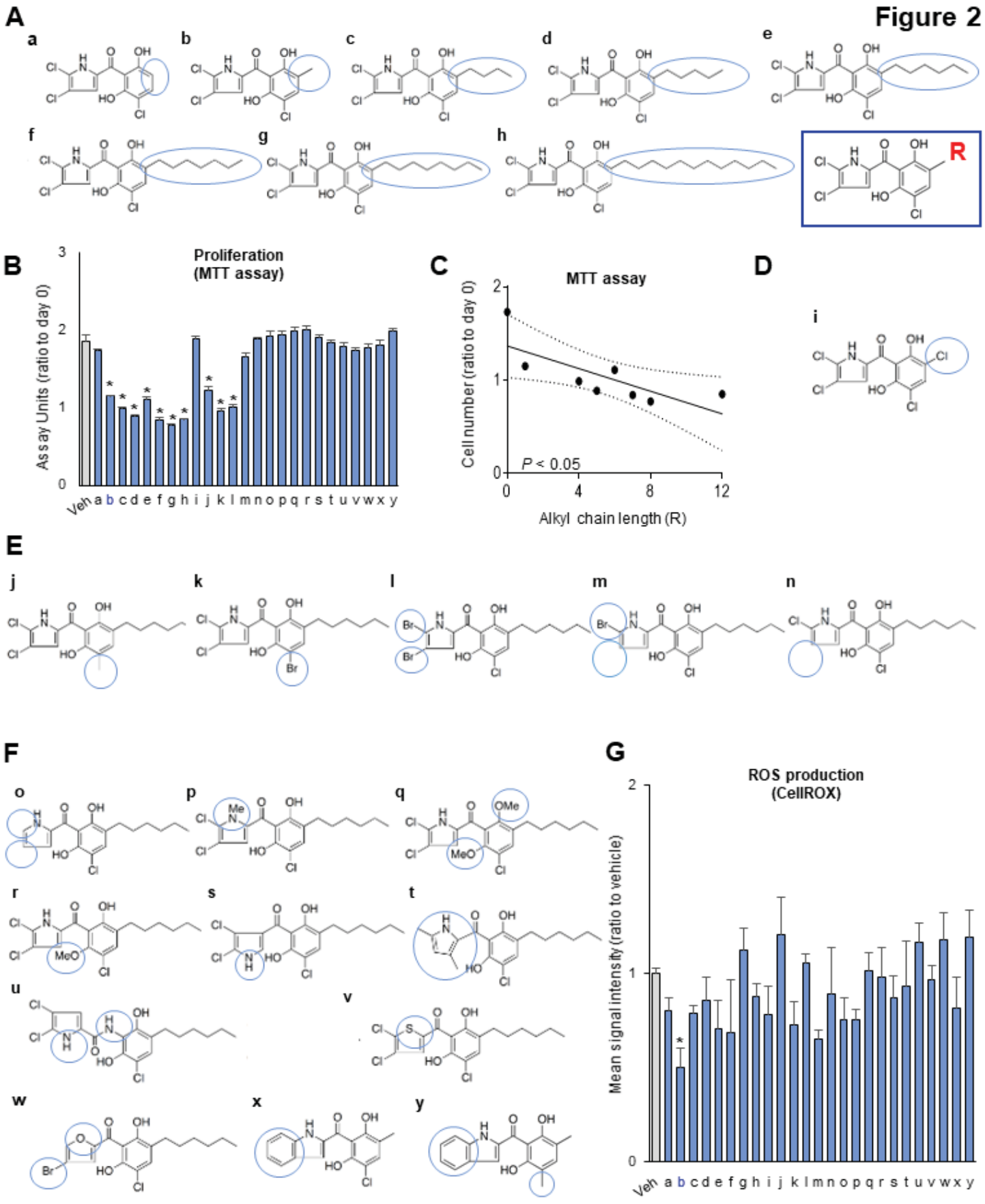

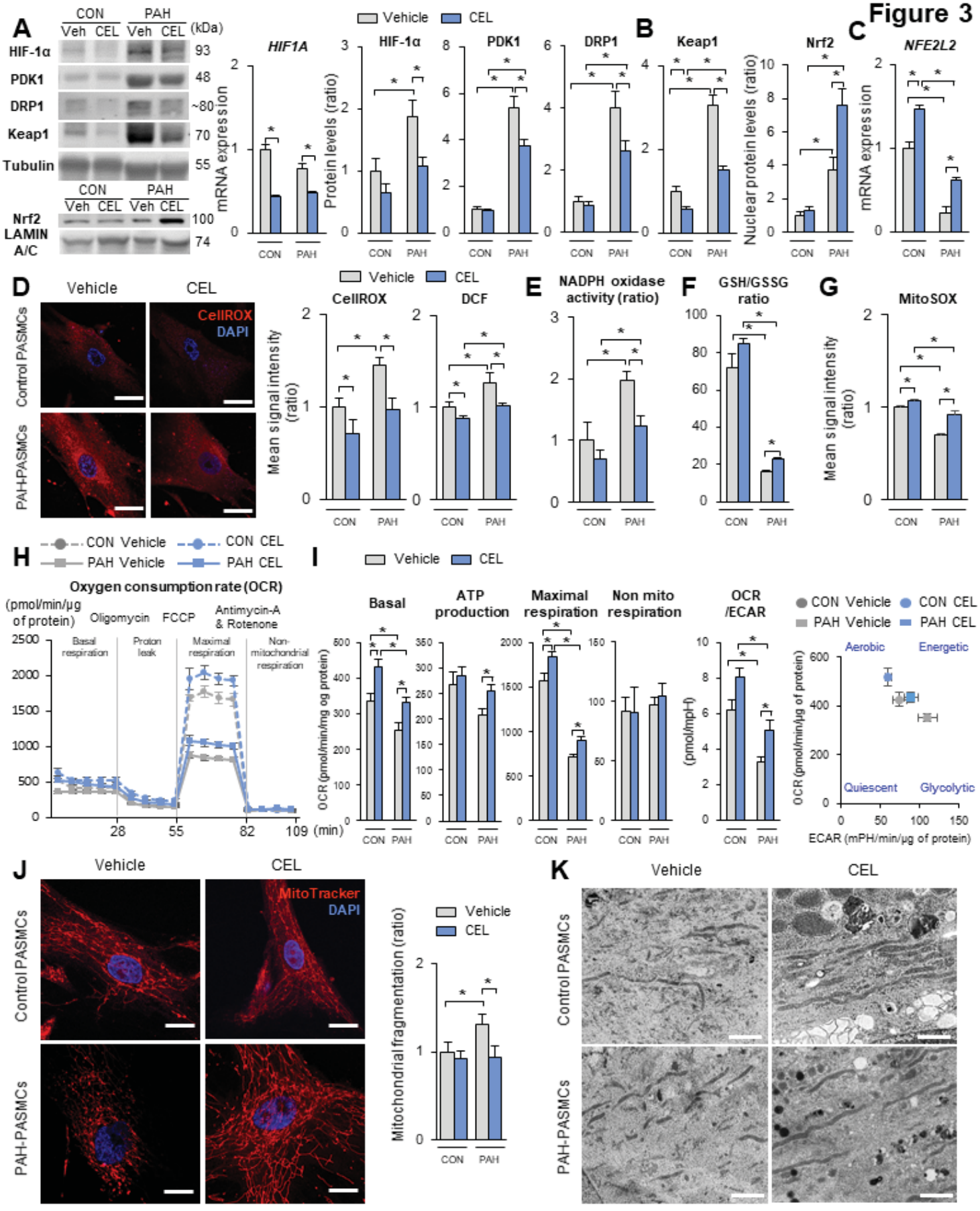

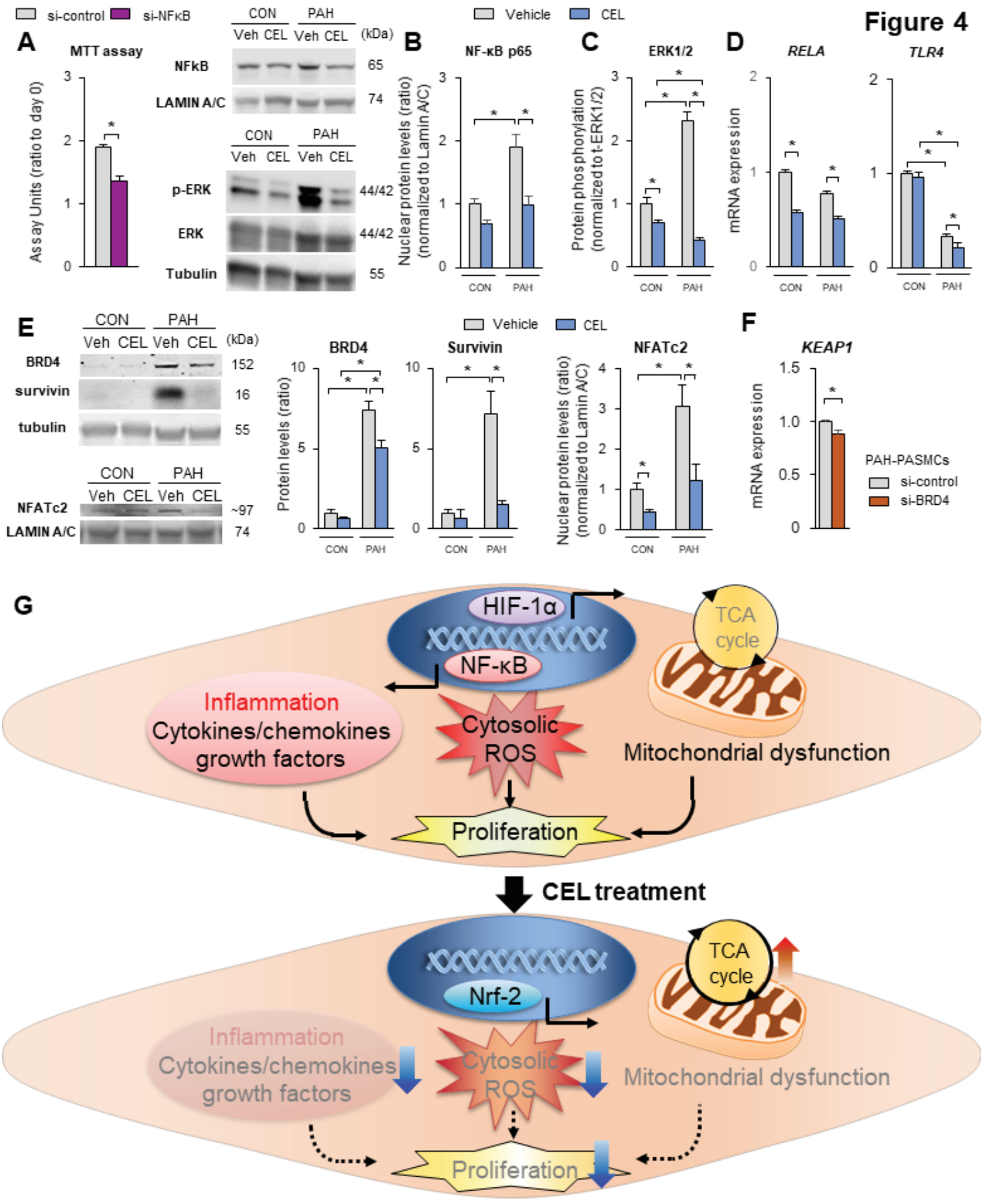

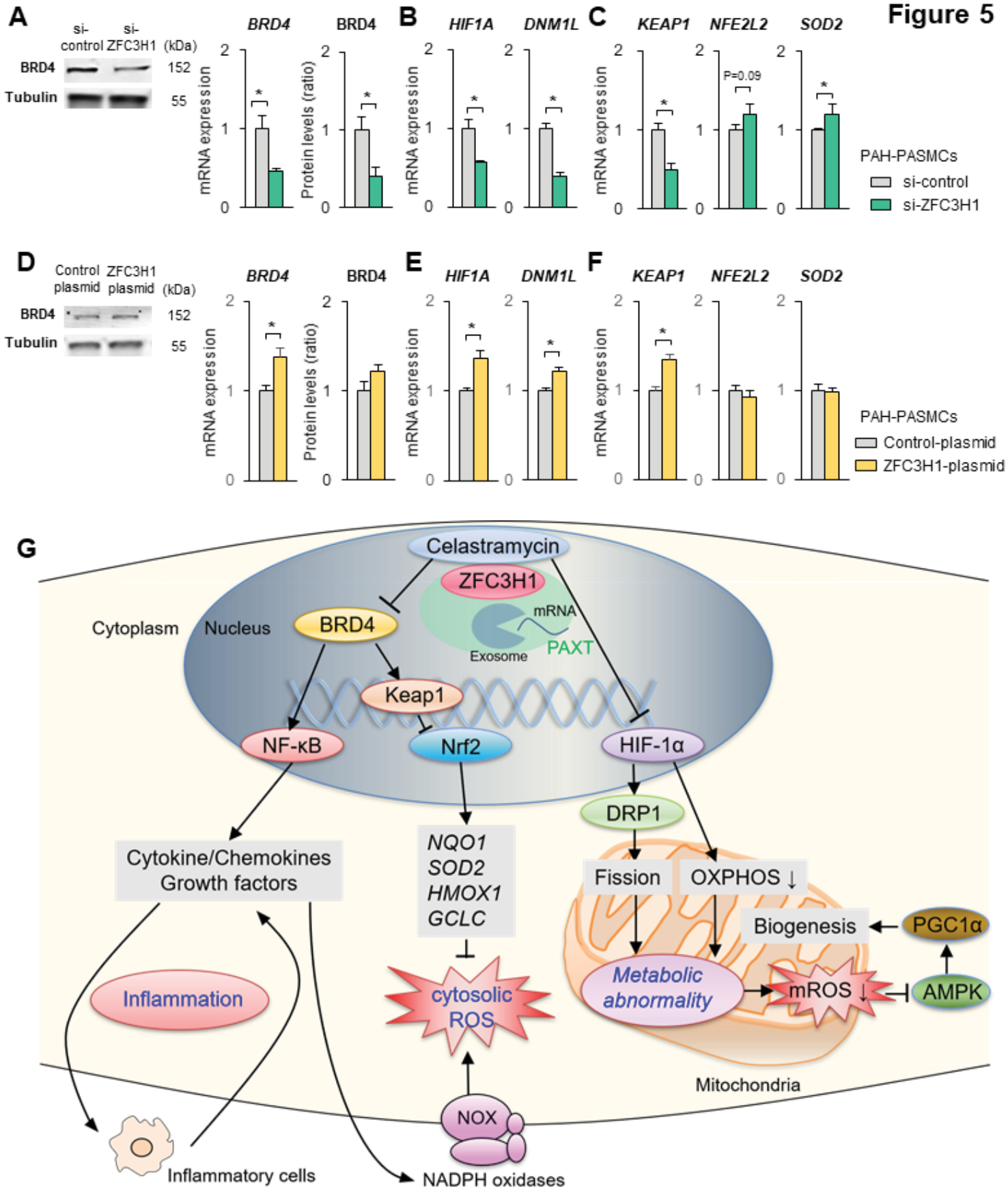

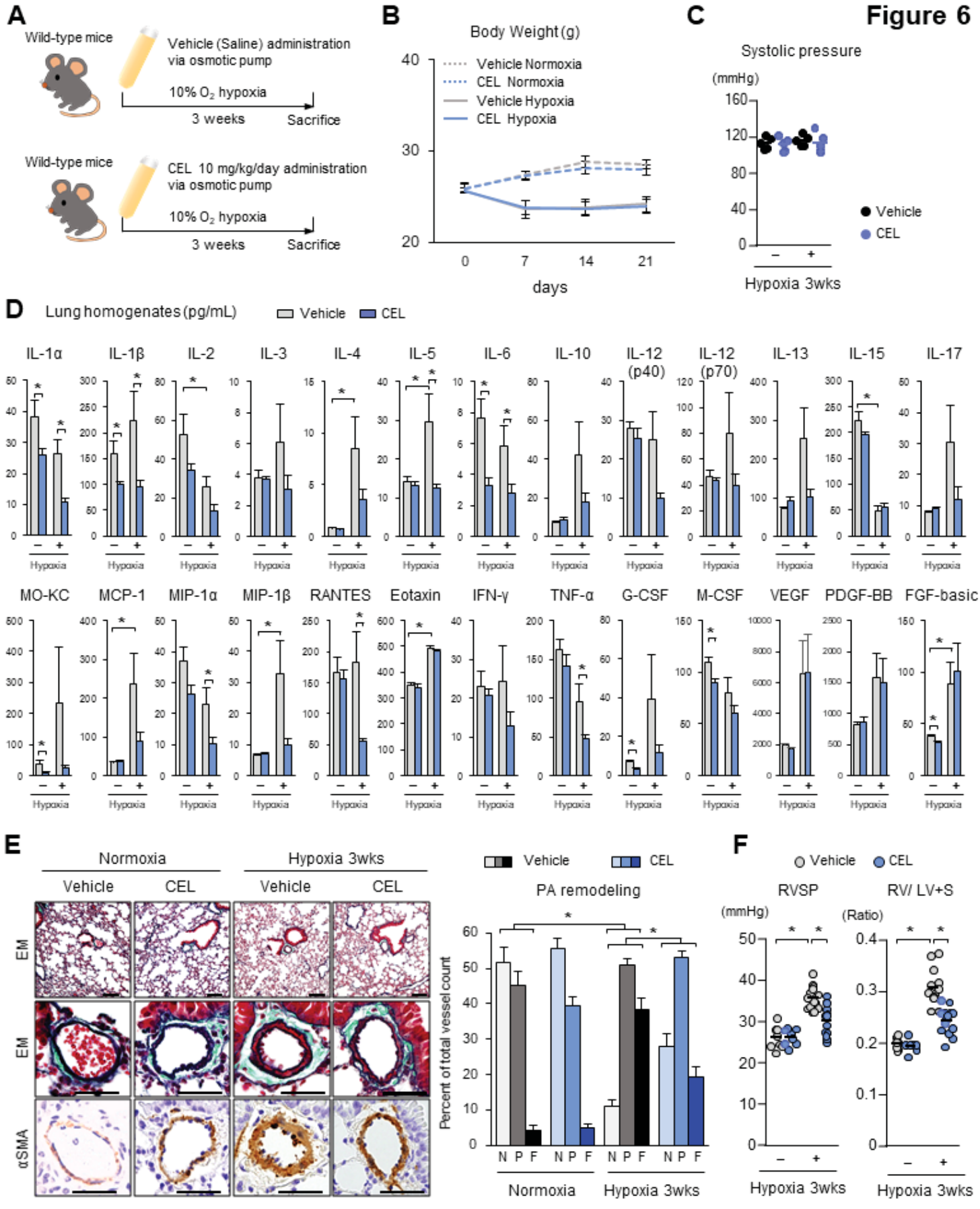

Figure 7